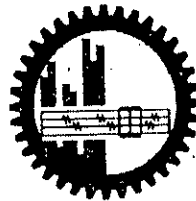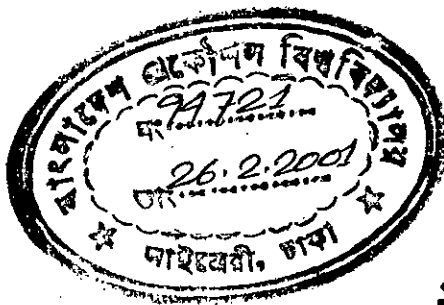# HEAT TRANSFER PERFORMANCE OF

INTERNALLY FINNED TUBE

Aloke Kumar Mozumder

Department Of Mechanical Engineering
Bangladesh University Of Engineering & Technology
Dhaka, Bangladesh

January 2001

HEAT TRANSFER PERFORMANCE OF INTERNALLY FINNED TUBE

By

Aloke Kumar Mozumder

A Thesis Submitted to the Department of mechanical Engineering in partial fulfillment of the requirements for the degree of
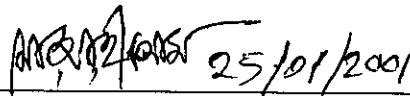
Master of Science

in

Mechanical Engineering

Department Of Mechanical Engineering
Bangladesh University Of Engineering & Technology
Dhaka, Bangladesh
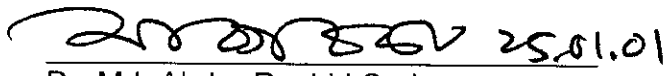
RECOMMENDATION OF THE BOARD OF EXAMINERS

The board of examiners hereby recommends to the Department of Mechanical Engineering, BUET, Dhaka, the acceptance of this thesis, **"Heat Transfer Performance of Internally Finned Tube,"** submitted by **Aloke Kumar Mozumder**, in partial fulfillment of the requirements for the degree of Master of Science in Mechanical Engineering.

Chairman (Supervisor)   :   _25/01/2001_
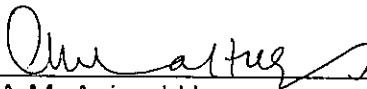
Dr. Md. Ashraful Islam
Assistant Professor
Department of Mechanical Engineering
BUET, Dhaka, Bangladesh.

Member (Ex-officio)   :   _25.01.01_

Dr. Md. Abdur Rashid Sarkar
Professor & Head
Department of Mechanical Engineering
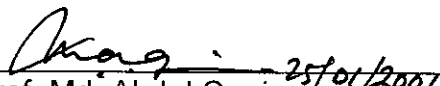BUET, Dhaka, Bangladesh.

Member   :   _25/01/2001_

Dr. A.M. Aziz-ul-Huq
Professor
Department of Mechanical Engineering
BUET, Dhaka, Bangladesh.

Member   :   _25/01/2001_

Prof. Md. Abdul Quaiyum
Professor
AMA International University
Dhaka, Bangladesh.

III

ABSTRACT

Heat transfer performance of a T-section internal fin in a circular tube has been experimentally investigated. The T-section finned tube was designed, fabricated and installed and was heated electrically. The same was done for a smooth tube in order to make comparison. Fully developed steady state turbulent airflow acts as a heat sink in this study. Data were collected in the Reynolds number range of 2.0×10^4 to 5.0×10^4 for smooth tube and 2.2×10^4 to 4.5×10^4 for finned tube. Wall temperature, bulk fluid temperature, pressure drop along the axial distance of the finned and smooth tube were recorded for the above mentioned Reynolds number. From the measured data, heat transfer coefficient, Nusselt number, friction factor and pumping power variation were calculated and analyzed.

Friction factor and pumping power are substantially increased in the finned tube in comparison to the smooth tube. For finned tube, friction factor is 3.0 to 4.0 times and pumping power is 3.5 to 4.5 times higher than those of smooth tube for the Reynolds number range 2.0×10^4 to 5.0×10^4. Heat transfer coefficient for finned tube is about 1.5 to 2.0 times higher than that of smooth tube in these Reynolds numbers. Higher heat transfer area may be one of the reasons for this heat transfer enhancement. The finned tube in this study produces significant heat transfer enhancement at the cost of increased pumping power.

ACKNOWLEDGEMENT

The author is highly grateful and indebted to his supervisor, Dr. Md. Ashraful Islam, Assistant Professor, Department of Mechanical Engineering, BUET, Dhaka, for his continuous guidance, supervision, inspiration, encouragement, and untiring support throughout this research work.
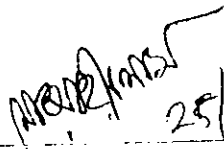
The author is also grateful to Dr. M. A. Rashid Sarkar, Professor & Head, Department of Mechanical Engineering, BUET, Dhaka, for his continuous assistance at different stages of this work.

The author expresses his thankfulness to Dr. A. M. Aziz-ul Huq, Professor, Department of Mechanical Engineering, BUET, Dhaka, for his valuable suggestions, sincere co-operation at all stages of this work.

Finally, the author likes to express his sincere thanks to all other Teachers and staffs of the Mechanical Engineering Department, BUET, Welding Shop and Machine Shop of BUET and BITAC, Dhaka for their co-operations and helps in the successful completion of the work.

DECLERATION

No portion of the work contained in this thesis has been submitted in support of an application for another degree or qualification of this or any other University or Institution of learning.

25/01/2001

Dr. Md. Ashraful Islam
Supervisor

25.01.2001

Aloke Kumar Mozumder
Author

CONTENTS

Nomenclature

A_f	Cross sectional area of fin (m^2)
A_h	Effective perimeter of finned tube (m)
A_s	Effective perimeter of smooth tube (m)
A_x	Cross sectional area of smooth tube (m^2)
A_{xf}	Cross sectional area of finned tube (m^2)
b	Atmospheric pressure head (in mm of Hg)
B	Bias limit of uncertainty
C_p	Specific heat of air (kJ/kgC)
d	Velocity head at inlet section (in cm of water)
D_h	Hydraulic diameter (m)
D_I	Inside diameter of tube (m)
F	Friction factor
H	Height of fin (mm)
h	Surface heat transfer co-efficient (W/m^2 ^{o}C)
k	Thermal conductivity of air (W/m^{o}C)
L	Length of the tube (m)
M	Mass flow rate (kg/s)
N	Number of fins
P	Pressure (N/m^2), precession limit of uncertainty
P_1	Inlet static pressure (N/m^2)
Q	Rate of heat transfer (W)

Q'	heat input to the air per unit area (W/m^2)
R	Inner radius of the tube (m), performance parameter (-)
ω	Specific gravity
t	Room temperature (°C)
T	Temperature (°C)
v	Kinematic viscosity (m^2/s)
V	Mean velocity in finned tube and smooth tube (m/s)
V$_i$	mean velocity in inlet section (m/s)
W	Total uncertainty
W	Width of fin (mm)
W$_f$	Wetted perimeter of fin (m)
W$_{ft}$	Wetted perimeter of finned tube (m)
x	Axial distance (m)
μ	Co-efficient of viscosity of air (N.s/m^2)
ρ	Density of air (kg/m^3)
ΔP	Pressure drop along axial length (N/m^2)

Subscripts

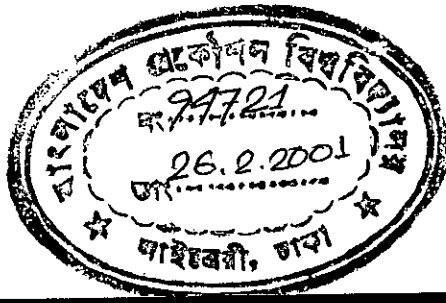|	
b	Bulk temperature
f	Finned tube
h	Based on hydraulic diameter
i	inlet
o	outlet
s	Smooth (unfinned) tube
w	Wall temperature
x	Axial distance

Dimensionless Numbers

Nu	Nusselt number = hD_h / K
Pr	Prandtl Number = $\mu C_p / K$
Re	Reynolds Number based on inside diameter = $\rho V D_i / \mu$

LIST OF FIGURES AND TABLES

INTRODUCTION

Most of the burgeoning research effort in heat transfer is devoted to analyzing what might be called the "standard situation". However, the development of high-performance thermal systems has also stimulated interest in methods to improve heat transfer. Improved heat transfer is referred to as heat transfer enhancement, augmentation, or intensification.

Enhancement techniques can be classified as passive methods, which require no direct application of external power, or active methods, which require external power. The effectiveness of both types depends strongly on the mode of heat transfer, which might range from single-phase free convection to dispersed-flow film boiling. Description of enhancement techniques are given below:

Passive Techniques:

i.   *Treated surface:* It involves fine-scale alternation of the surface finish or coating (continuous or discontinuous). It is used for boiling and condensation; the roughness height is below that which affects single-phase heat transfer.

ii.   *Rough surface:* These surfaces are produced in many configurations, ranging from random sand-grain type roughness to discrete protuberances. The configuration is generally chosen to promote turbulence rather than to increase the heat transfer surface area. The application of rough surfaces is directed primarily toward single-phase flow.

iii.   *Extended surface:* These are routinely employed in many heat exchangers. The

development of non-conventional extended surfaces, such as integral inner fin tubing, and the improvement of heat transfer coefficients on extended surfaces by shaping or interrupting the surface as of particular interest.

iv. *Swirl-flow device:* It includes a number of geometric arrangements or tube inserts for liquid flow that create rotating and/or secondary flow such as inlet vortex generator, twisted-tape insert and axial-core inserts with a screw-type winding.

v. *Coiled tube:* It leads to more compact heat exchangers. The secondary flow leads to higher single-phase coefficients and improvements in most regions of boiling.

Active Techniques:

i. *Mechanical aids:* These stir the fluid by mechanical means or by rotating the surface.

ii. *Surface vibration:* At either low or high frequency, surface vibration has been used primarily to improve single-phase heat transfer.

iii. *Fluid vibration:* It is the most practical type of vibration enhancement. The vibrations range from pulsation of about 1 Hz to ultrasound. Single-phase fluids are of primary concern.

iv. *Fluid injection:* It involves supplying of gas to a flowing liquid through a porous heat transfer surface or injecting similar fluid upstream of the heat transfer section.

Two or more of these techniques may be utilized simultaneously to produce an enhancement larger than that produced by only one technique. This simultaneous use is termed compound enhancement.

Extended surfaces are commonly used in many engineering applications to enhance heat transfer. A number of studies are being performed in order to increase the heat transfer effectiveness and to reduce the dimensions and weight of heat exchangers. The necessity to reduce the volume and weight of heat exchanger has become more important in many engineering applications like electronic industry, compact heat exchanger sector. Fins have

extensive applications in power plants, chemical process industries, and electrical and electronic equipment for augmentation of heat transfer. Enhancement techniques that improve the overall heat transfer coefficient of turbulent flow in tubes are important to heat exchanger designers. Efficient design of heat exchanger with fins can improve system performance considerably. Among several available techniques for augmentation of heat transfer in heat exchanger tubes, the use of internal fin appear to be very promising method as evident from the results of the past investigations.

Extensive studies have been made both experimentally and analytically with tubes having internal fins in laminar and turbulent flow. A comprehensive survey in this regard is chronologically given in the Chapter. 2. The analysis for laminar and turbulent flow is based on momentum and energy conservation in the flowing fluid. It is evident that for both laminar and turbulent flow regimes, the finned tube has exhibited substantially higher heat transfer coefficient compared to smooth (unfinned) tubes.

Since finned surfaces have extensive applications in various engineering sectors; present work has been undertaken to study the heat transfer performance in turbulent flow regime of air in a circular tube with finned and unfinned conditioned. Fins are specially designed with a view to getting better heat transfer compared to the internal fins ever studied. Specific objectives of the present study are listed below:

i. to study the variation of friction factor, pressure drop and temperature through smooth tube and finned tube at constant heat flux, and

ii. to analyze the heat transfer performance of the finned tube.

3

LITERATURE SURVEY

Enhancement techniques that improve the overall heat transfer coefficient for both laminar and turbulent flow in tubes are important to heat exchanger designers. It is evident that for both laminar and turbulent flow regimes, the finned tubes have exhibited substantially higher heat transfer coefficients when compared with corresponding smooth (unfinned) tubes.

Extensive studies have been performed from the beginning of the twentieth century to determine the heat transfer characteristics inside tubes. Sieder and Tate (1936) derived an empirical correlation for turbulent flow of forced convection through both of circular and noncircular tube, as

$$\overline{Nu}_D = 0.027 Re_D^{0.8} Pr^{0.3} \left(\frac{\mu_b}{\mu_s} \right)^{0.14} \qquad (2.1)$$

where Nu_D is average nusselt number based on hyrdaulic diameter, Re_D is Reynolds number based on hydraulic diameter, Pr is Prandtl number, μ is viscosity of flowing fluid and the subscripts b and s indicates at bulk temperature and surface temperature respectably. This co-rrelation is valid for both uniform wall temperature and uniform heat flux for both liquid and gases in the range of $0.7 < Pr < 16,000$ and $Re_D > 6000$. The correlation shows that higher heat transfer occurs in finned tube than smooth one. Heat transfer with disturbing the flow (as interrupted, cut and twisted perforated etc.) geometry has been used by Gunter and

Shaw (1942). Experimental data for pressure drop and heat transfer coefficient for air in internally finned tubes have been reported by Hiding and Coogan (1964). All studies show higher coefficients in disturbed flow than smooth one.

Cox et al. (1970) used several kinds of enhanced tube to improve the performance of a horizontal-tube multiple-effect plant for saline water conversion. Overall heat transfer co-efficient (forced convection condensation inside and spray-film evaporation outside) were reported for tubes internally enhanced with circumferential V grooves (35% maximum increase in heat transfer co-efficient) and protuberances produced by spiral indenting from the outside (4% increase). No increase was obtained with a knurled surface. Prince (1971) obtained 200% increase in heat transfer co-efficient with internal circumferential ribs; however, the outside (spray-film evaporation) was also enhanced. Experimental data for pressure drop and heat transfer coefficient in internally finned tubes have been reported by Bergles et al. (1971). Most of their data are characterized by the laminar flow regimes using air, water and oil as working fluids. Enhanced fins (interrupted and perforated) were used by Kern and Kraus (1972). They demonstrated that finned tubes have substantially higher heat transfer coefficients than continuous finned tubes.

Hu and Chang (1973) analyzed fully developed laminar flow in internally finned tubes by assuming constant and uniform heat flux in tube and surfaces. By using 22 fins extended to about 80% of the tube radius, it is shown an enhancement of heat transfer as high as 20 times than that of unfinned tube.

Nandakumar and Masliyah (1975) analyzed heat transfer characteristics for a laminar forced convection of fully developed flow in a circular tube having internal fins of circular shape with axially uniform heat flux with peripherally uniform temperature using a finite element method. They obtained for a given fin geometry that the Nusselt number based on inside diameter was higher than that of a smooth tube. They also found that for maximum heat transfer there exists an optimum fin number for a given fin configuration. Heat transfer and pressure drop measurements were made by Watkinson et al. (1975) on integral inner-fin tubes of several designs in laminar oil flow. Data are presented for eighteen 12.7 to 32 mm diameter tubes containing from 6 to 50 straight or spiral fins over the Prandtl number range of 180 to 250, and the Reynolds number range of 50 to 3000, based on inside tube diameter

and nominal area. At constant pumping power and the same Reynolds number, the increase in heat transfer ranged from 100% to 187%.

Glodsterin and Sparrow (1976) have studied some complex compact heat exchanger surfaces using mass transfer methods, for example naphthalene sublimation. Internally finned tubes can be stacked to provide multiple internal passages of certain hydraulic diameter.

The first analytical study to predict the performance of tubes with straight internal fin in turbulent airflow was conducted by Patankar et al. (1979). The mixing length in the turbulent model was set up so that just one constant was required from experimental data. Analytical efforts to fluids of higher Prandtl number, tubes of perfectly circular and tubes with spiral fins is still desirable. Random roughness consisting of attached metallic particle (50% area density and relative roughness 0.03%) was proposed by Fenner and Ragi (1979). He obtained 300% higher heat transfer with R-12 compared to smooth tube.

Empirical correlations have been presented by Carnavos (1980). He predicted the turbulent flow heat transfer and pressure loss performance of helical ribbed internal finned tube within acceptable limits for air in the overall ranges of $0 < \alpha$ (helix angle of rib) $< 30^{\circ}$, $10,000 < Re < 100,000$, and $0.7 < Pr < 30$. There is no strong indication that these types of tubes are Prandtl number sensitive. However, there is an indication that the spiral fin tubes deviate the most from the slope of 0.8, which becomes more pronounced at the higher helix angles and lower Reynolds numbers. The best performers were in the group of tubes with the higher helix angles and internal heat transfer surface relative to a smooth tube. He experimentally determined the heat transfer performance for cooling air in turbulent flow in tubes having integral internal spiral and straight longitudinal fins. He conducted experiments with 21 tubes and found that these tubes were potentially capable of increasing the capacity of an existing heat transfer at constant pumping power by 12% to 66% by direct substitution of an internal finned tube for a smooth tube.

Compact heat exchangers have large surface-area-to-volume ratios primarily through the use of finned surfaces. An informative collection of articles related to the development of compact heat exchanger is presented by Shah et al. (1980). Compact heat exchangers of the

plate-fin, tube and plate-fin, or tube and center variety use several types of enhanced surfaces: offset strip fins, lowered fins, perforated fins, or wavy fins were presented by Shah (1980) .Circular or oval finned-tube banks utilize a variety of enhanced surfaces, with the exception of material pertaining to smooth helical fins, data are rather limited and no generalized correlations presently exist. Webb (1980) provides a guideline to such types of geometry.

Gee and Webb (1980) have presented experimental investigations of offset-fin arrays for air. The effect of plate thickness on heat transfer for two-dimensional staggered fin arrays have been studied numerically by Prakash and Patankar (1981). They also investigated the influence of buoyancy on heat transfer in vertical internally finned tube under fully developed laminar flow condition.

Numerical predictions of developing fluid flow and heat transfer in a circular tube with internal longitudinal continuous fins have been reported by Chowdhury and Patankar (1985) and Prakash and Liu (1985) who used air as the working fluid. Kelkar and Patankar (1987) also analyzed internally finned tubes numerically, whose fins are segmented along their length. The fin segment was done in the flow direction, separated by an equal distance of its length before the next fin. The analysis presents that the inline-segmented fin gives only 6% higher Nusselt number than those of continuos fins. Rustum and Soliman (1988) carried out analyses of thermally developed laminar flow in internally finned tubes for incompressible Newtonian fluid.

Edwards et al. (1994) performed an experimental investigation of fully developed, steady and turbulent flow in a longitudinal finned tube. They used a two-channel, four beam, laser-doppler velocimeter to measure velocity profiles and turbulent statistics of airflow seeded with titanium dioxide particles. They compared friction factor with different Reynolds numbers to literature results and showed good agreement for both smooth and finned tubes.

Mafiz et al. (1996, 1998) studied experimentally steady state turbulent flow heat transfer performance of circular tubes having six integral internal longitudinal fins and they found an abrupt pressure fluctuation near the entrance region of the tube. Their study indicates that

significant enhancement of heat transfer is possible by using internal fins without scarifying additional pumping power. The author used air as the working fluid.

Uddin (1998) studied pressure drop characteristics and heat transfer performance of air through an internal rectangular finned tube. He found that the heat transfer co-efficient based on inside diameter and nominal area was in the range of 1.5 to 1.75 times the smooth tube values. When compared with a smooth tube at constant pumping power and constant basic geometry of the tube an improvement as high as 4% was obtained. Mamun (1999) studied pressure drop and heat transfer performance of air through an internally in line segmented and non-segmented finned (of rectangular cross section) tube at constant pumping power. The results of the study show that friction factor of in-line finned tube is 2.0 to 3.5 times higher than that of smooth tube. Friction factor of in-line segmented finned tube is 1.75 to 2.5 times higher than that of smooth tube. Heat transfer for the in-line-finned tube is two times higher than that of smooth tube for comparable Reynolds number. Heat transfer for the in-line segmented finned tube is 1.75 to 2.0 times higher than that of smooth tube for comparable Reynolds number. The results thus show that both inline finned tube and in-line segmented finned tube results in heat transfer enhancement but in-line segmented finned tube results in the same heat transfer enhancement with less pressure drop and with less pumping power.

In line with the above mentioned studies in heat transfer in finned tube, present geometry was chosen in search of better heat transfer and lower pumping power. Details of the present experimental scheme will be discussed in chapter 4.

HEAT TRANSFER PARAMETER

In this chapter the basic definition of heat transfer parameters and thermal boundary conditions in connection with the present work have been discussed. The hydraulic diameter and wetted perimeter of the test section, Reynolds number, pressure drop, friction factor, amount of heat transfer, bulk temperature, heat transfer coefficient, pumping power etc. are presented here in mathematical form.

3.1 THERMAL BOUNDARY CONDITION

Appropriate boundary and initial conditions are needed for the analysis of heat transfer problems. The boundary conditions specify the thermal condition at the boundary surfaces of the region. The boundary conditions may be defined by its temperature condition, heat flux condition, convective boundary condition etc. In this work constant heat flux boundary condition is considered. In mathematical form this condition may be defined as:

$$q(x,0) = constant.$$

where q is heat flux, x is axial direction of the tube and 0 is angular position the tube.

3.2 HYDRAULIC DIAMETER

For internal fluid flows the hydraulic diameter, D_h is usually used as characteristic length. It

is defined as four times the cross section area of conduit per unit wetted perimeter. As such, the D_h for smooth tube is defined as

$$D_h = \frac{4 \times \left(\pi D_i^2 / 4 \right)}{\pi D_i}$$

$$\Rightarrow D_h = D_i \tag{3.1}$$

And for finned tube it can be expressed as

$$D_h = \frac{4 \times A_{xf}}{W_{ft}} \tag{3.2}$$

$$\text{where}, \ A_{xf} = \frac{\pi}{4} D_i^2 - 6 \times A_f$$

$$W_{ft} = \pi D_i - 6 \times W + 6 \times W_f$$

$$W_f = \text{wetted perimeter of fin}$$

$$W = \text{width of fin}$$

3.3 REYNOLDS NUMBER

Reynolds number is the ratio of inertia force to viscous force. It is a dimensionless number and used as a criterion for a flow to be laminar or turbulent. For circular pipe flow the Reynolds number less than 2.3×10^3 is laminar flow and greater than this is turbulent flow. In this experiment Re is used as an important parameter.

Reynolds number based on inside diameter is defined as

$$Re = \frac{\rho V D_i}{\mu} \tag{3.3}$$

Reynolds number based on hydraulic diameter is defined as

$$Re_h = \frac{\rho V D_h}{\mu}$$

(3.4)

3.4 PRESSURE DROP AND FANNING FRICTION FACTOR

Pressure drop is hydraulic loss due the roughness of the surface over which the fluid is moving. Higher pressure drop requires higher pumping energy for flowing of a fluid over a surface. For rough surface the drop of pressure is high. So pressure drop at any axial location x is given by the following equation,

$$\Delta P = P_i - P(x)$$

(3.5)

where P_i = Pressure at inlet

$P(x)$ = Pressure at any axial location, x

The local friction factor based on hydraulic diameter is given by

$$F_h = \frac{(-\Delta P / x)D_h}{2\rho V^2}$$

(3.6)

The local friction factor based on inside diameter is given by

$$F_i = \frac{(-\Delta P / x)D_i}{2\rho V^2}$$

(3.7)

3.5 HEAT TRANSFER RATE

Heat transfer rate is the energy transfer to the air per unit time. Total heat input to the air

$$Q = MC_p (T_o - T_i)$$

(3.8)

11

For smooth tube, heat input to the air per unit area

$$Q' = MC_p (T_o - T_i) / A_s L \qquad (3.9)$$

The local bulk temperature of the fluid $T_b(x)$ can be defined as by the following heat balance equation

$$T_b(x) = T_i + \frac{Q' A_s x}{MC_p} \qquad (3.10)$$

The local heat transfer coefficient at any axial location can be defined as

$$h_x = \frac{Q'}{(T_w - T_b)_x} \qquad (3.11)$$

The average heat transfer coefficient can be defined as

$$\bar{h} = \frac{Q}{A(T_w - T_b)_{av}} \qquad (3.12)$$

For finned tube, heat input to the air per unit area

$$Q' = MC_p (T_o - T_i) / A_h L \qquad (3.13)$$

The local bulk temperature of the fluid $T_b(x)$ can be defined by the following heat balance equation

$$T_b(x) = T_i + \frac{Q' A_h x}{MC_p} \qquad (3.14)$$

The local heat transfer coefficient at any axial location can be defined as

$$h_x = \frac{Q'}{(T_w - T_b)_x} \qquad (3.15)$$

The average heat transfer coefficient can be defined as

$$\bar{h} = \frac{Q}{A(T_{wav} - T_{bav})}$$ (3.16)

Local Nusselt number based on inside diameter (for both smooth and finned tube)can be defined as

$$Nu_x = \frac{h_x D_i}{K}$$ (3.17)

3.6 PUMPING POWER

Pumping power, P_m can be expressed as $= \frac{\Delta P}{\rho} . M$ (3.18)

3.7 PERFORMANCE PARAMETER

There are minor geometric differences in tube configuration among various experiments that affect specific performance. However to minimize the influence of this and other variables on a direct comparison, the basis chosen is the constant Reynolds number criterion. In this criterion, the performance parameter, R is defined as the ratio of heat transfer coefficient with fin, h_f to the heat transfer coefficient without fin, h_{of} at constant Reynolds number.

So,

$$R = h_f / h_{of}$$ (3.19)

EXPERIMENT

Experimental facility and procedure for collecting the heat transfer data for both smooth and finned tube are described in this chapter. The experimental ranges are also mentioned here. Uncertainty estimates of the measurands and the calculated variables are also presented in this chapter.

4.1 EXPERIMENTAL RIG

Test section is the heart of the experimental rig, which is schematically shown in the Fig. 4.1. The rig is provided with inlet section for getting fully developed airflow in the test section. Air supply system and heating system are the other essential parts of the rig with a view to fulfil the objectives of this study. The overall dimension of the rig is given in Fig. 4.2. The experiment has been conducted between the range of Reynolds number of 2.0×10^4 and 5.0×10^4. All the sections of the rig are described below.

4.1.1 Test Section

Two test sections having two different geometries have been studied to compare their heat transfer performance. One tube is smooth and other is finned. Smooth tube is a circular brass tube having 70 mm inside diameter. While the finned tube is one having six internal longitudinal T-section fins as shown in Fig.4.3. The test length of both the tubes is 1500

mm. Similar casting methods are employed for both the pipes for getting comparable properties. Two halves of the circular tube with integral fins were casted separately and joined together to provide the shape of a complete tube. As the two halves were joined together at the line of symmetry, it did not provide any effect on thermal or hydrodynamic performance.

All the test sections were wrapped at first with mica sheet and then glass fiber tape before wrapping with Nichrome wire (of resistance 0.249 ohm/m for smooth tube and 0.739 ohm/m for finned tube used as an electric heater) spirally wound uniformly with spacing of 16 mm around the tube. Then again mica sheet, glass fiber tape, heat insulating tape and asbestos powder were used sequentially over the wrapped Nichrome wire. The test section was placed in the test rig with the help of the bolted flanges, between which asbestos sheets were inserted to prevent heat flow in the longitudinal direction.

4.1.2 Inlet Section

The unheated inlet section (shaped inlet) cast from aluminium is of same diameter as of test section. An open end of the pipe would probably act as a sharp edged orifice and air flow would contract and not fill the pipe completely within a short distance from the end. This effect was avoided here in the experiment by fitting a shaped inlet. The pipe shaped inlet, 533 mm long (shown in the Fig. 4.4) was made integral to avoid any flow disturbances at upstream of the test section to get fully developed flow in the test section as well. The coordinates of the curvature of the shaped inlet were suggested by Owner and Pankhurst (1977).

4.1.3 Air Supply System

A motor operated suction type fan was fitted downstream the test section to supply air that will cool the test section for ascertaining the heat transfer performance. A suction type fan was used here so that any disturbance produced by the fan does not effect on the test section flow, as a suction type fan is always fitted at the down stream side of the test section. A 12° diffuser made of mild steel plate is fitted to the suction side of the fan. The diffuser was used

15

for minimizing head loss at the suction side. To arrest the vibration of the fan a flexible duct was installed between the inlet section of the fan and a gate valve as shown in Fig. 4.2. The gate valve is of butterfly type and was used to control the flow rate of air. It is fitted at the suction side before the flexible duct.

4.1.4 Heating System

An electric heater (made of Nichrome wire) was used to heat the test section at constant heat flux. The heater was supplied power by a 5 KVA variable voltage transformer connected to 220 VAC power through a magnetic contactor and temperature controller. The Nichrome wire was wrapped around the test piece as shown in Fig. 4.2. A temperature controller was fitted to sense the outlet air temperature to provide signal for switching the heater off or on automatically. It protects the experimental set up from being excessively heated which may happen at the time of experiment when the heating system is in operation continuously for hours to bring the system in steady state condition. It also controls the air outlet temperature. Electric heat input by Nichrome wire was kept constant for all the experiments.

The electrical power to the test section was determined by measuring the current and voltage supplied to the heating element. The voltage was measured with a voltmeter and current by an a.c. ammeter. Figure 4.5 shows the electric circuit diagram of the heating system of the test section. The specification of the electric heater, temperature controller and fan are given in Appendix-A.

4.2 MEASUREMENT SYSTEM

Different variables were measured by different types of instruments, some of those were manually operated and some were automatically. The detail description of all the systems used in this study are described in the following sections.

4.2.1 Flow Measuring System

Flow of air through the test section was measured at the inlet section with the help of a traversing pitot. A shaped inlet was installed (as mentioned in the section 4.12) at the inlet to

the test section to have an easy entry and symmetrical flow. The traversing pitot was fitted at a distance of 4D, from the inlet according to Owner and Pankhurst (1977). The manometric fluid used here is high-speed diesel of specific gravity 0.855. A schematic of the micrometer traversing pitot is shown in Fig. 4.6. Arithmetic mean method (given in Appendix-C) is employed to determine the position of the pitot tube for determination of mean velocity.

4.2.2 Pressure Measuring System

The static pressure tappings were made at the inlet of the test section as well as equally spaced 8 axial locations of the test section as shown in the Fig. 4.8. Pressure tappings for measurement of static pressure were fitted so carefully that it just touches the inner surface of test section. The outside parts of the tappings were made tapered to ensure an airtight fitting into the plastic tubes, which were connected to the manometer. Epoxy glue was used for proper fixing of the static pressure tappings. U-tube manometers at an inclination of 30° were attached with the pressure tapping. Water was used as the manometric fluid in this experiment.

4.2.3 Temperature Measuring System

The temperatures at the different axial locations of the test section were measured with the help of K-type thermocouples connected with a data acquisition system as shown in Fig. 4.1. The data acquisition system stored data at five minutes interval for obtaining an average value. The temperature measuring locations are-

  i.   Fluid bulk temperature at the outlet of the test section.
  ii. Wall temperature at 8 axial locations of the test section.
  iii. Fin-tip temperature at 8 axial locations of the test section. This measurement was done when finned tube was set in the test rig.

The bulk temperature of the air at the outlet of the test section was measured using a thermocouple at the outlet of the test section to determine the locations of thermocouple for determination of mean temperature. It is given in Appendix-C.

17

For smooth tube heat transfer system, 8 thermocouples were fitted at eight equally spaced axial locations of the test section one at each position to measure the wall temperature. Thermal contact between the brass tube and the thermocouple junction was assured by peening thermocouples junction into grooves in the wall. Thermocouples were inserted into the holes and peened into the gooves of the tube wall. For finned tube system, sixteen thermocouples were fitted at eight locations as shown in the Fig. 4.10. The number of thermocouples was two in each cross section to measure the wall as well as the fin-tip temperature of the test section.

4.3 EXPERIMENTAL PROCEDURE

The fan was first switched on and allowed to run for about five minutes to have the transient characteristics died out. The flow of air through the test section was set to desired value and kept constant with the help of a flow control valve. Then the electric heater was switched on. The electrical power was adjusted (if necessary) with the help of a regulating transformer or variac. Steady state condition for temperature at different locations of the test section was defined by Gee and Webb (1980) by two measurements. First the variation in wall thermocouples was observed until constant values were attained, then the outlet air temperature was monitored. Steady state condition was attained when the outlet air temperature did not deviate over 10-15 minutes time. At the steady state condition thermocouple readings are automatically recorded by the data acquisition system. At the same time, manometer readings were taken manually.

After each experimental run the Reynolds number was changed with the help of the flow control valve keeping electrical power input constant. And after waiting for steady state condition, desired data are recorded as per procedure narrated above.

4.4 UNCERTAINTY ANALYSIS

Results of an uncertainty analysis of the primary measurands (t, b, d, A, T_o, T_i, ΔP, D_i, x) are presented in Table 4.1, while Table 4.2 exhibits the uncertainites of the calculated quanties.

Table 4.1 Uncertainties in measurands

Measurands	Precision limit, P	Bias limit, B	Total limit, W
t	1.5%	0.02%	1.50%
b	0	0.013%	0.013%
d	1.05%	3.0%	3.178%
A	0	0.52%	0.52%
T_a	1.5%	0.02%	1.50%
T_i	1.5%	0.02%	1.50%
ΔP	5.0%	3.0%	5.83%
D_i	0	0.02%	0.02%
x	0	0.02%	0.02%

Table 4.2 Uncertainties in calculated quantities

Quantity	Total uncertainty
V	1.71%
Q	4.1%
F_i	6.76%

The details of the uncertainty analysis of this experiment are given in Appendix-D

Data Acquisition System

Thermocouple

Air in
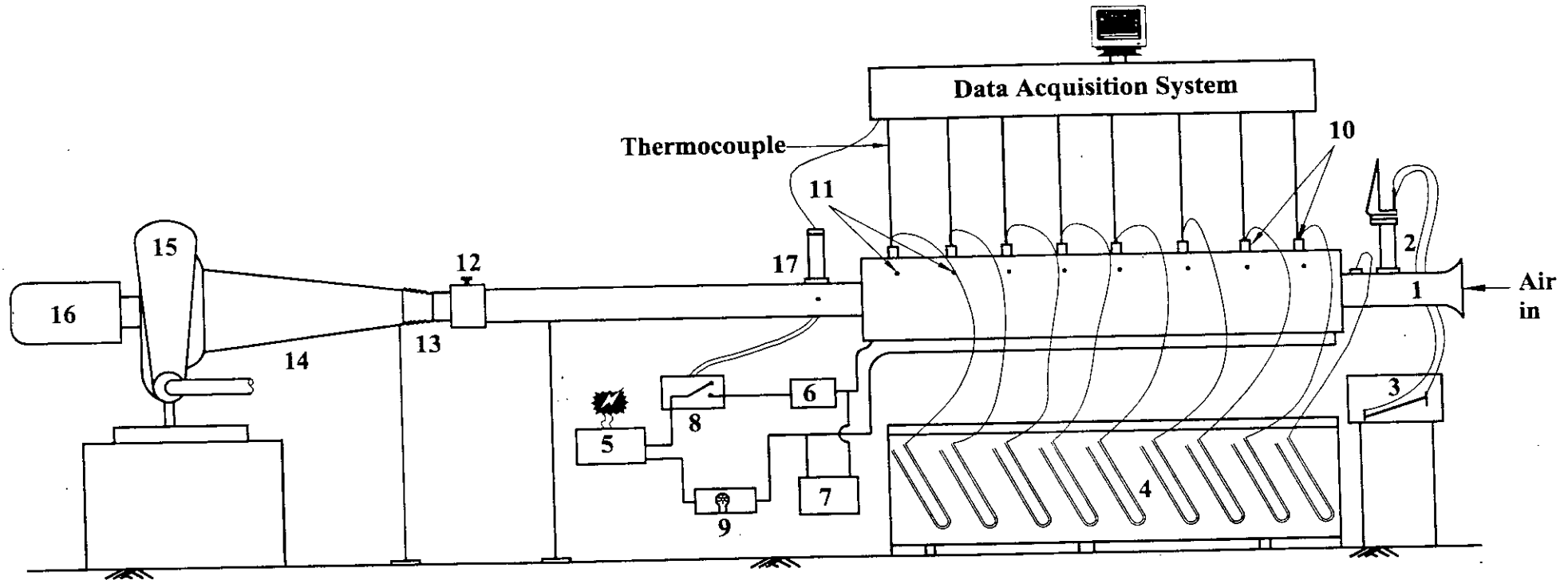
1.	Shaped inlet	6.	Ammeter	11.	Thermocouples	16.	Motor
2.	Traversing pitot tube	7.	Voltmeter	12.	Flow conrtol valve	17.	Traversing thermocouple
3.	Inclined tube manometer	8.	Temperature controller	13.	Flexible pipe		
4.	U-tube manometer	9.	Heater on off lamp	14.	Diffuser		
5.	Variable voltage Transformer	10.	Pressure tappings	15.	Fan		

FIGURE 4.1: Schamatic of the Experimental Rig

20
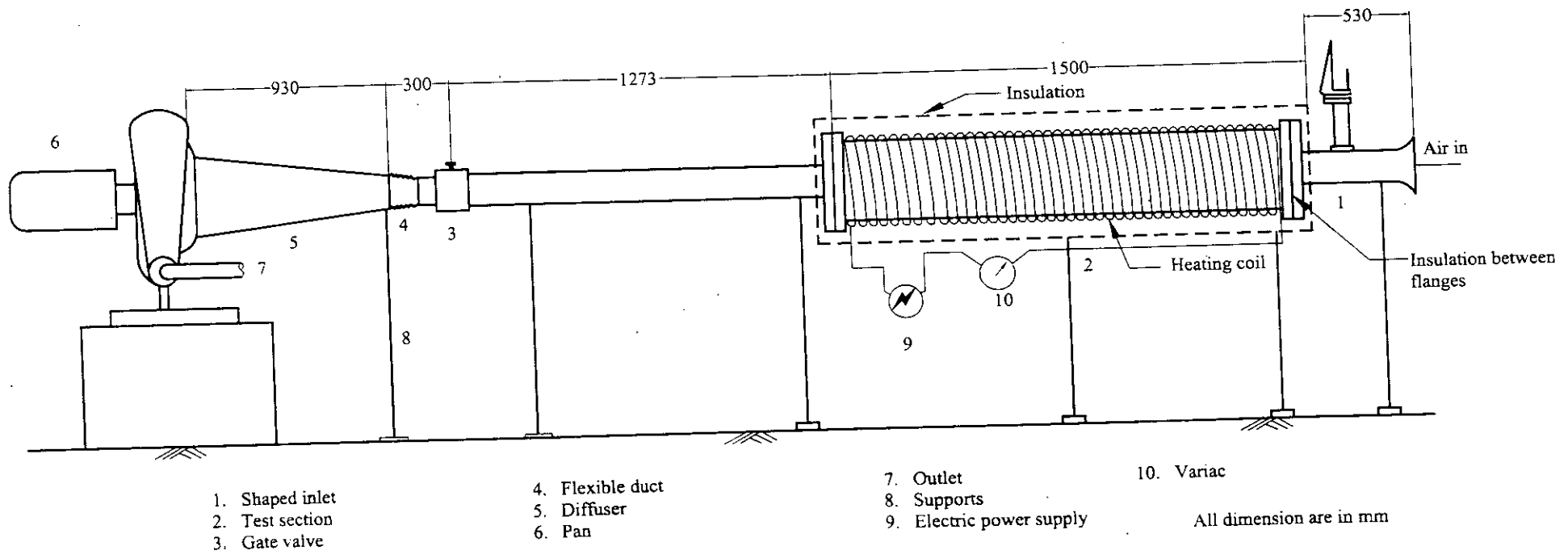
FIGURE 4.2: SCHEMATIC DIAGRAM OF EXPERIMENTAL SET UP WITH DIMENSIONS

1. Shaped inlet
2. Test section
3. Gate valve
4. Flexible duct
5. Diffuser
6. Pan
7. Outlet
8. Supports
9. Electric power supply
10. Variac

All dimension are in mm
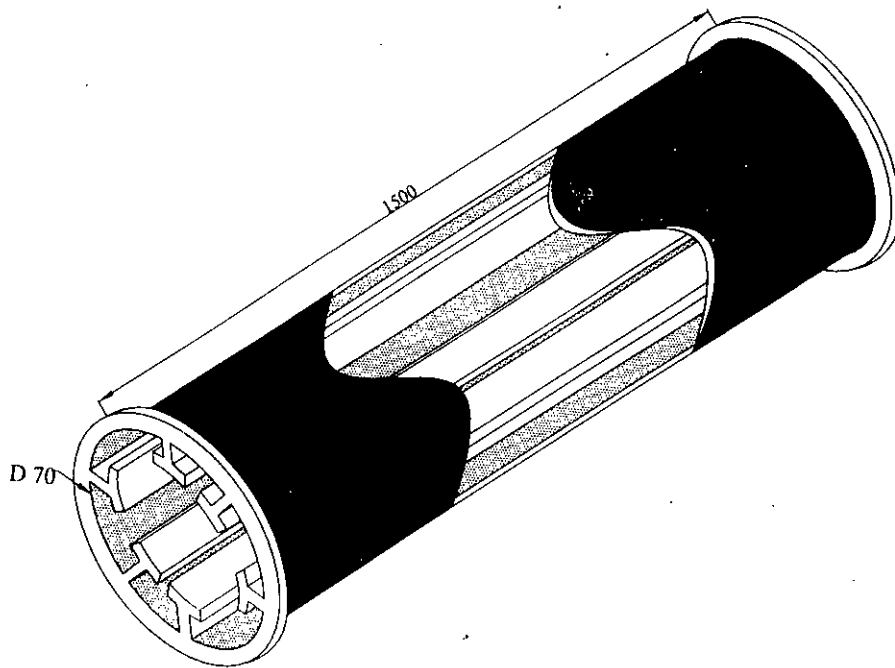
(a) 3-DIMENSIONAL VIEW OF THE TEST SECTION
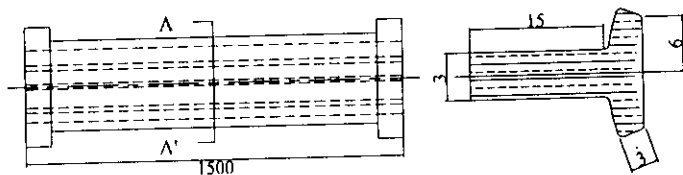
(b) FRONT VIEW

(c) T-SECTION
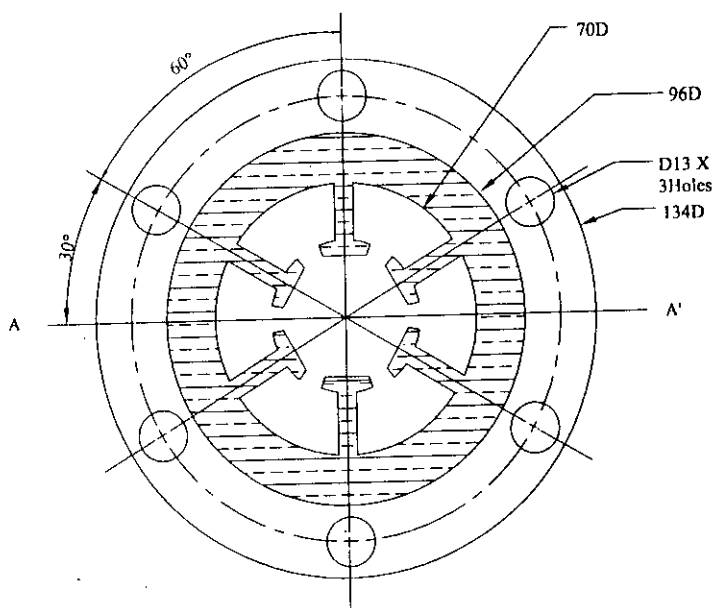
(d) VIEW A-A'

Figure 4.3:   Test Section and its cross sectional view

FIGURE 4.4: SHAPED INLET

C_1 ~ Temperature controlloer
C_2 ~ Magnetic controller
S ~ Switch
V ~ Voltmeter
A ~ Ammeter
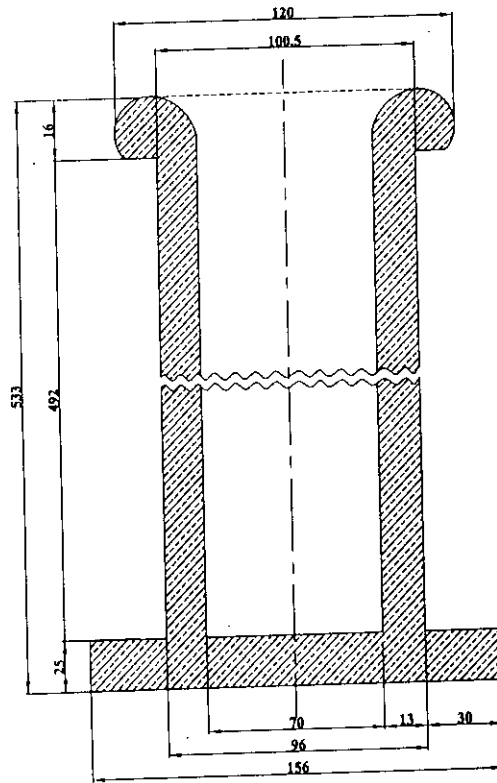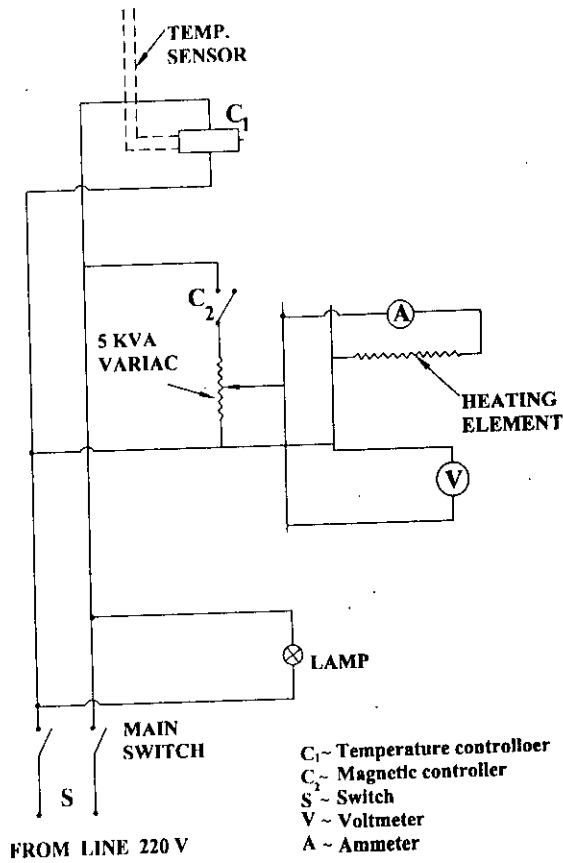
FIGURE 4.5: ELECTRICAL CIRCUIT DIAGRAM
FOR HEATING SYSTEM

Thread

38

1.5

9

4.5

13

19

13

Rectangular groove

3 mm hole

Thread

6

38

13

13

9

3

233

213

245

194

26

16

15

15

64

All dimensions are in mm
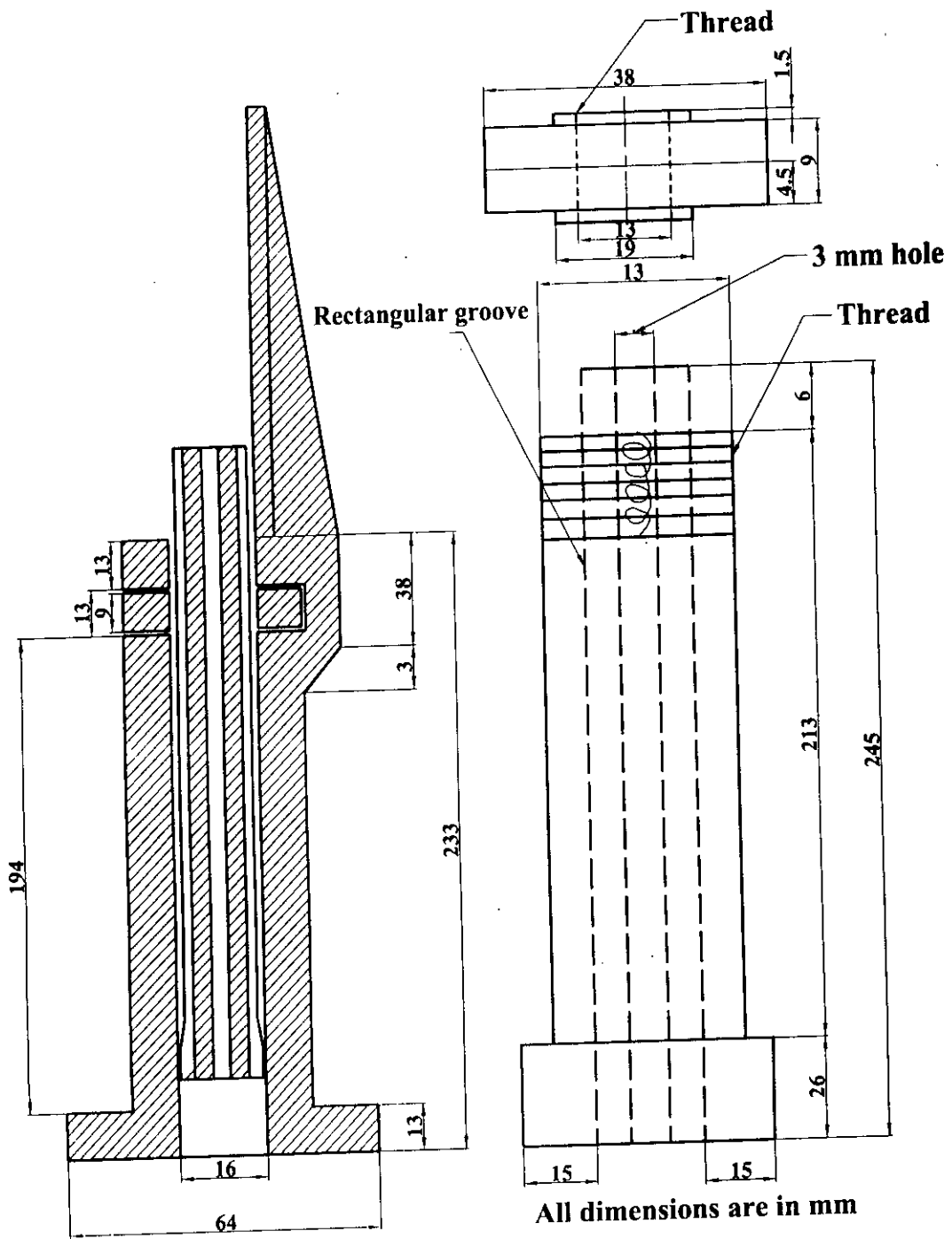
FIGURE 4.6: TRAVERSING PITOT TUBE HOLDING DEVICE

24
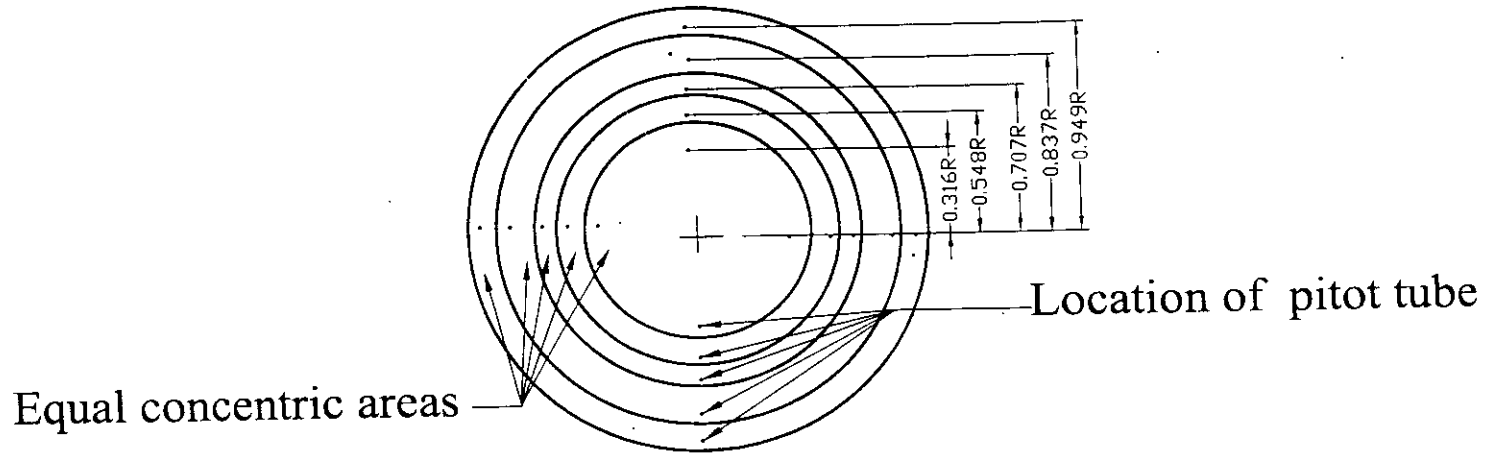
Figure 4.7 Location of pitot tube for Measurement of Velocity
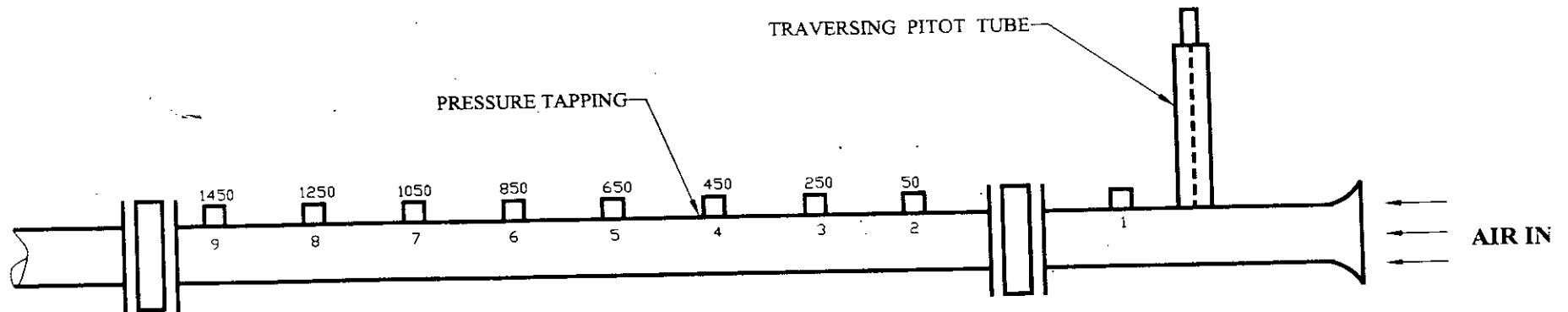
Figure 4.8 Location of Pressure Tapping
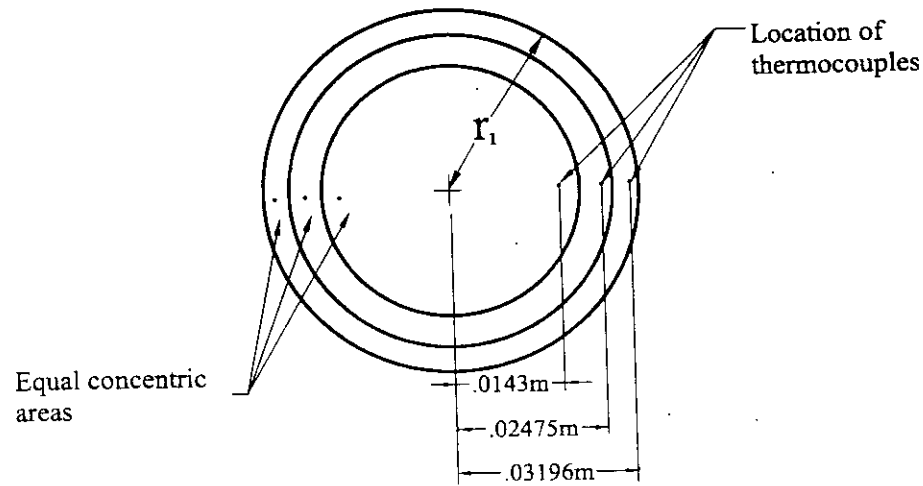
Figire 4.9 : Location of Thermocouplefor Measurement of outlet Temperature

w ~ wall
f ~ Fin
i ~ Inlet
o ~ Outlet
a ~ Air
C ~ Coupling/Flange

Tao ~ Air outlet temp
Tc ~ Temp. at the flange
Tw2 ~ wall temp at 2
Tf2 ~ Fin-tip temp at 2
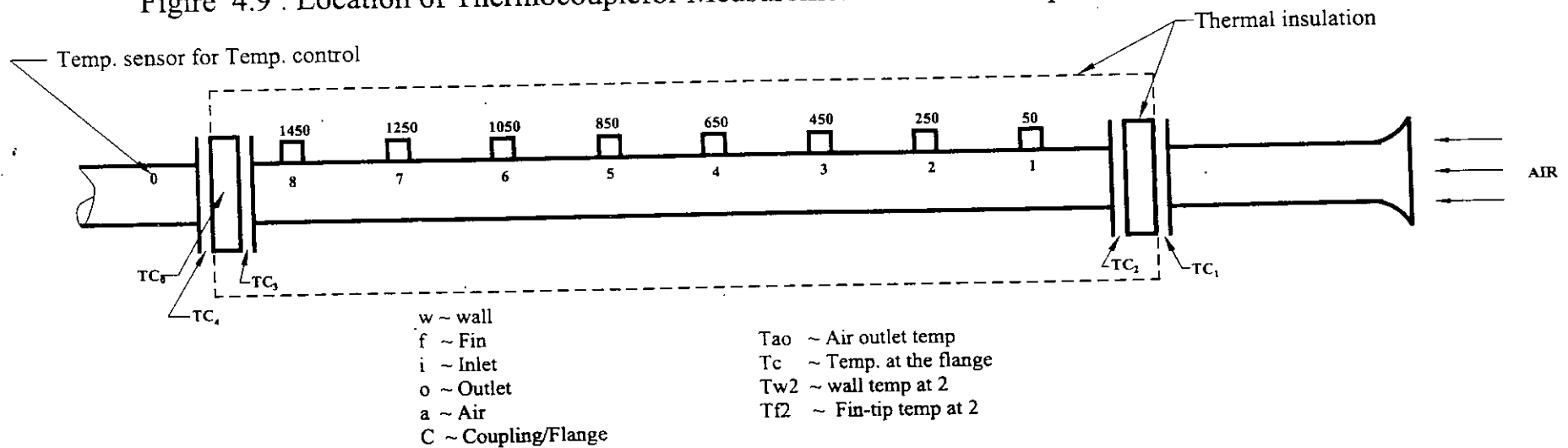
Figure 4.10   Location of Thermocouples

26

RESULTS AND DISCUSSION

Heat transfer performance study of fin has been carried out by recording temperature and pressure along the length of the tube at each experimental condition, which was set by a constant heat input and fluid flow. Airflow is also measured at each test run. All the necessary variables have been calculated from the collected data and are presented and analyzed in this chapter.

5.1 TEMPERATURE DISTRIBUTION

Wall temperature, bulk fluid temperature and fin tip temperature variation along the length of the tube for different Reynolds Number are presented in Figs. 5.1-9 to understand the mechanism of heat transfer.

5.1.1 Wall Temperature

Figure 5.1 shows the variation of wall temperature along the length of the smooth tube for five different Reynolds numbers at constant heat flux condition. Each symbol represents data for a particular Reynolds number as shown in the figure. The axial position of any point is non-dimensionalized by the total length of the tube. From the figure it is clear that wall temperature increases along axial distance of the test section. At about x/L = 0.55, the wall

temperature gets its maximum value while for x/L = 0.55 to 0.85 the temperature is almost constant, after which the temperature drops slightly at the downstream due to end effect. The end effect may be due to the physical contact (though there was two asbestos plates between the test section and the down stream unheated tube, which may not enough for unexpected heat loss) between the test section and the down stream unheated tube. Figure 5.1 also shows that air cools the tube much faster at higher Reynolds number.

Figure 5.2 represents the variation of wall temperature along the length of the finned tube for five different Reynolds numbers at constant heat flux condition. Here wall temperature increases along the axial distance of the test section. At higher Reynolds number the wall temperature is low because more heat is taken away by air. It is worth mentioning that at inlet section the temperature gradient is high for both the tubes because the cold entering air takes away much heat. It is interesting to note that unlike smooth tube there is a gradual increase in wall temperature for the finned tube. Figure 5.3 exhibits this clearly for a comparable Reynolds Number as mentioned. Due to higher heat transfer from the inner surface of the finned tube the wall gets cooled. As smooth tube has lower wetted perimeter and less mixing situation due to smaller frictional area it has no such ability to transfer heat as quickly as does the finned tube. As a result the wall gets heated when it is smooth.

Figure. 5.4 shows the variation of fin-tip temperature along the axial distance of the tube. From this figure it is clear that the tip temperature of fin varies in the similar manner as in the case of wall temperature mentioned above. The slope of these curves gradually decreases along the axial distance. Because the temperature potential between air and the fin tip becomes lower with longitudinal distance of the tube. A comparison between tip and wall temperature of finned tube is given in Fig. 5.5, which demonstrates that wall temperature is always higher than that of fin tip for a particular Reynolds Number.

It is necessary to mention that before experiment, the radial temperature distribution was checked at different axial location of the test section. Figure 5.6 represents the variation of temperature around the outer surface i.e. over the insulation of the test section for both tubes at X/L ~ 0.83. At top portion the temperature is higher than bottom. Due to natural convection top portion of the test section becomes more heated, so its temperature is higher. From the figure it is also clear that for smooth tube the temperature is higher than finned

28

tube. Because a lower amount of heat was transferred to the working fluid in smooth tube, so relatively higher amount of heat was bound to transfer through the insulation provided the insulating condition is same for both the tubes. As more heat was passed through the insulating surface the surface temperature of the smooth tube is higher than finned tube.

5.1.2 Bulk Fluid Temperature

Surrounding cold air enters the test section and gets heated as it passes through it. The bulk fluid temperature is calculated from the measured wall temperature using Eq. (3.10). The bulk fluid temperature variation along the length of the test section is shown in Figs. 5.7-9 in order to get effects of Reynolds number and fin as well. From Fig. 5.7, for constant Reynolds number. it is clear that bulk fluid temperature increases linearly as air passes through the test section of smooth tube. Similar behavior also observed for the case of finned tube as shown in Fig. 5.8. At higher Reynolds number the bulk fluid temperature is lower. The slope of these curves (dT/dx) gradually decreases with the increase of Reynolds number. Because at lower Reynolds number there is less velocity of air which provides enough time for sufficient heating of air but at higher Reynolds number faster moving of air makes it insufficient heating and thus it is relatively cold for a constant axial position.

Figure 5.9 represents the variation of bulk fluid temperature distribution along the length of the tubes for comparable Reynolds number for both finned and smooth tube. From the figure it is clear that for smooth tube the bulk fluid temperature is lower than that of finned tube. Due to higher transfer of heat from the inner surface of the tube, the bulk temperature is higher in finned tube. But smooth tube has lower wetted perimeter and less mixing of fluid in it than finned tube. So smooth tube has no such ability to transfer of heat as quickly as finned tube and so its air bulk temperature is lower.

5.2 HEAT TRANSFER CHARACTERISTICS

The variation of heat transfer coefficient and Nusselt number along the axial direction of the tube (finned and smooth) for different Reynolds numbers are explained in this section. A

comparison of these parameters of heat transfer for finned and smooth tube is also discussed here.

5.2.1 Heat Transfer Coefficient

Both local and average heat transfer coefficients are calculated and analyzed here. Figure 5.10 shows the variation of local heat transfer co-efficient with axial direction of the smooth tube. The coefficient is large at the entrance of the test section due to the development of thermal boundary layer. The coefficient decreases continuously along the axial distance up to X/L = 0.42 after which the thermal boundary layer could be considered as fully developed. After X/L = 0.8 value of the heat transfer coefficient increases a little, as such a drop in temperature is observed as shown in Fig. 5.1.

Figure 5.11 represents the variation of local heat transfer co-efficient with axial direction of the finned tube. The coefficient is large at entry of the test section as observed for smooth tube. But the developed region starts earlier than observed in smooth tube. Here the developing region ended at X/L = 0.3. It is occurred due to better heat transfer in finned tube.

Figure 5.12 shows the variation of heat transfer rate as function of different Reynolds number for both finned and smooth tube. From the figure it is clear that heat transfer increases with increase of Re. At higher Re there is higher mixing of air, which helps to increase the heat transfer. The amount of heat transfer of finned tube is higher than that of smooth tube. The wetted perimeter of finned tube is higher than smooth tube, which helps to increase the rate of heat transfer.

Figure 5.13 shows the variation of average heat transfer coefficient based on D_i as a function of Reynolds number. Present data are compared with those of Uddin (1998), Mafiz et al. (1998), and Mamum (1999). The heat transfer coefficient data collected in this experiment is 2.5 to 3.5 times higher than that of data collected by Uddin (1998) for his inline rectangular fin geometry. It is about 1.5 to 2.0 times higher than that of data measured by Mafiz et al. (1998) for his inline rectangular fin geometry, Mamum (1999) for his inline segmented rectangular fin configuration and Mamum (1999) for inline rectangular fin geometry. From this comparison it can be inferred that heat transfer increases almost

Nusselt is about two times higher than that of Mamun (1999). The cause of variation of data with Sieder and Tate (1936) may be due to fact that the surface condition of the test section of Sieder and Tate (1936) was perfectly smooth tube, but in this work the tube was smoothed with zero grade emery paper. So this tube contains slightly granular surface. Due to this roughness of surface small higher heat transfer occurred. So all the experimental data from this work passes slightly above the line predicated by Sieder and Tate (1936). This comparison concludes that heat transfer increases almost linearly with Reynolds number i.e. disturbance of flow increases the rate of heat transfer.

5.3 FLUID FLOW CHARACTERISTICS

In this article pressure drop, friction factor and pumping power variation are presented along the longitudinal direction of the test section. All these parameters are presented here for both finned and smooth tube for five different Reynolds numbers. Comparison for different fin geometry for different pumping power is also made.

5.3.1 Pressure Drop

Figures 5.18 -19 represent the variation of pressure drops with axial distance for smooth and finned tube, respectively, with Reynolds number as a parameter. The pressure inside the tube is always negative because the test section is at suction side of the fan. If there is an ideal condition, pressure every where in the test section would be same, but due to frictional losses a pressure drop occurs along the axial direction of flow. The pressure gradient is high in the entrance region and gradually diminishes along the flow direction as shown in the figure. Figure 5.20 shows a comparison between smooth tube and finned tube on pressure drop characteristics for a comparable Reynolds Number. From this figure it is clear that for finned tube pressure drop is much higher than that of smooth tube. It is as high as four times compared to smooth tube for Re 2.9×10^4. This may be due to higher skin friction factor in the finned tube.

5.3.2 Friction Factor

Figures 5.21-22 represent the variation of friction factor with dimensionless distance for both finned and smooth tube. The friction factor is high near the entrance region, then sharply falls upto X/L = 0.3, after which it then remains almost constant. It can be noted that as the Reynolds number increases friction factor decreases. From the Fig. 5.23, it is worth mentioning that the friction factor becomes independent of Reynolds number at higher Reynolds number and remains constant after the value of $Re = 4.0 \times 10^4$. At the entrance region friction factor is high which may be due to settings of asbestos plate between the shaped inlet and test section. In this study it is observed that the friction factor is 2.0 to 7.0 times higher in finned tube than smooth tube. The higher frictional area is responsible for higher skin friction factor in finned tube.

A comparison has been made for experimental data for both finned and smooth tube with that of Mamun (1999) for in line finned tube. For all types of test section the friction factor is higher at the entrance section as shown in the Fig. 5.24. The cause may be due to the settings of asbestos plate explained earlier. The experimental data for finned tube is 3.0 to 4.0 times higher than those for smooth tube and 1.0 to 2.0 times higher for $Re = 2.9 \times 10^4$ than that of Mamun (1999). The higher frictional area contributes higher friction factor.

5.3.3 Pumping Power

Pumping power required for a fluid to pass through an internally finned tube is very important to be estimated in order to estimate the heat transfer performance of the tube. High heat transfer followed by less pumping power is always desirable. Figure 5.25 shows the variation of pumping power with Reynolds Number for both finned and smooth tube. From the figure it is seen that the pumping power of finned tube is much higher than that of smooth tube. It is about 4.5 times higher for $Re = 3.9 \times 10^4$ than that of smooth tube. Due to increase of wetted perimeter the frictional area increases which is responsible for higher pressure drop and consequently the pumping power increases. Figure 5.26 also shows a

comparison of pumping power of experimental data of finned tube with that of Mamun (1999). The value of pumping power of inline finned tube of Mamun (1999) is about 1.0 to 3.5 times higher and for inline segmented finned tube of Mamun (1999) is about 1.0 to 2.25 times higher than that of experimental value. It can be noted that the experimental friction factor value of finned tube is higher than that of Mamun (1999) as shown in the Fig. 5.24, but the pumping power is low, it is not yet clear what actually happened, it may due to smaller flow rate of air through the finned tube than that of Mamun (1999).

5.4 PERFORMANCE PARAMETER

The performance of a fin indicates whether a tube having fin provides better heat transfer and less pressure drop during its flow. The performance parameter of a finned tube is expressed as the ratio of heat transfer coefficient of test section with fin to that without fin. Figure 5.27 represents a comparison of performance parameter for experimental data with that of Mamun (1999). Its value is about 0.75 times less than that of inline finned tube of Mamun (1999) and about 0.9 times less than that of inline segmented finned tube of Mamun (1999). It may occur due to the fact that the smooth tube used in the present work was not perfectly smooth as explained earlier, which provides better heat transfer. Due to this higher heat transfer from smooth tube the ratio of h_f / h_{of} decraeses, though the heat transfer from finned tube is higher than that of Mamun (1999). It can be noted here that the surface properties of finned tube are similar to those of smooth tube. So due to roughness of surface, the heat transfer also increases in finned tube but relatively higher increase of h_{of} value the value of h_f / h_{of} decreases.

Figure 5.1: Wall temparature distribution along the length of the smooth tube
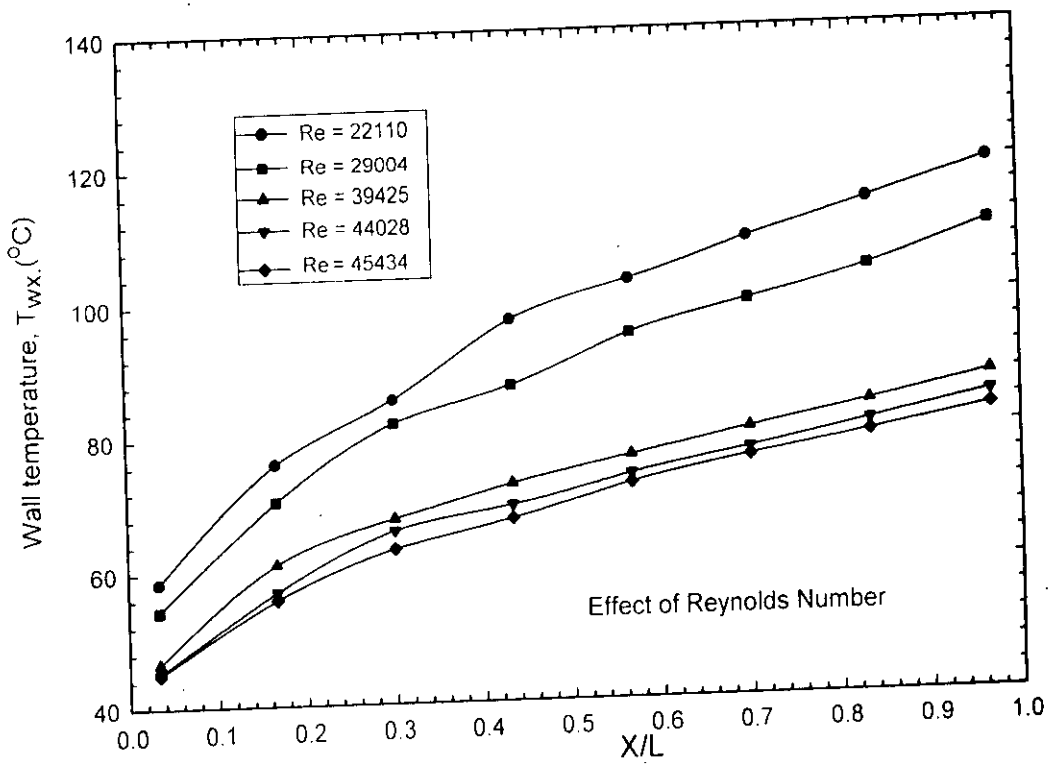
Figure 5.2: Wall temparature distribution along the length of the finned tube
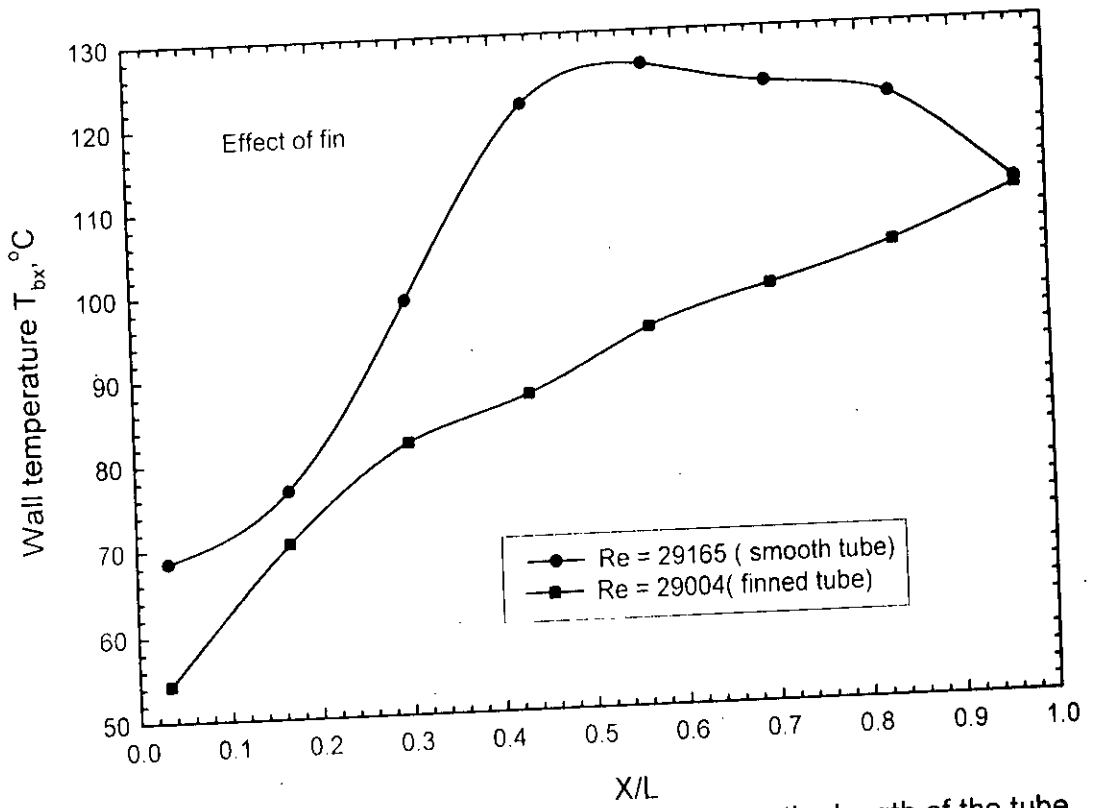
Figure 5.3 : Wall temperature distribution along the length of the tube
for compareable Reynolds number

Figure 5.4: Fin tip temparature along the length of the finned tube
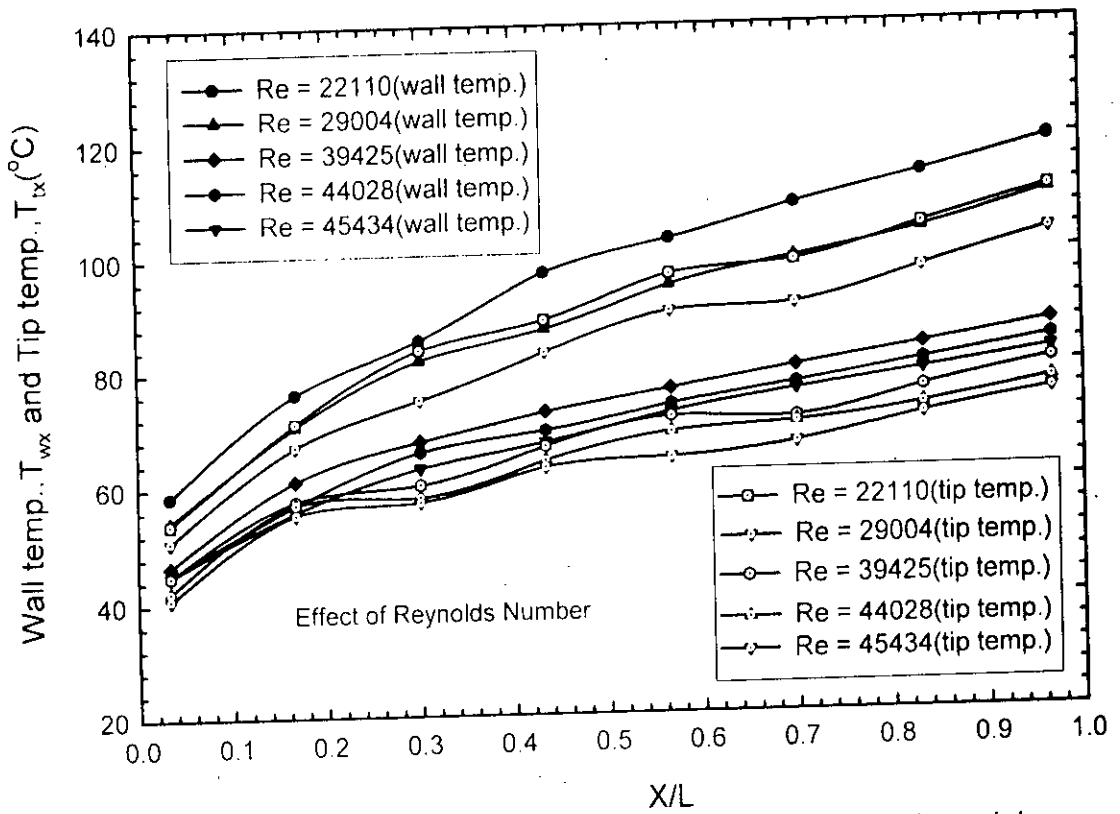
Figure 5.5: Comperism of wall and tip temp. along the axial direction of finned tube
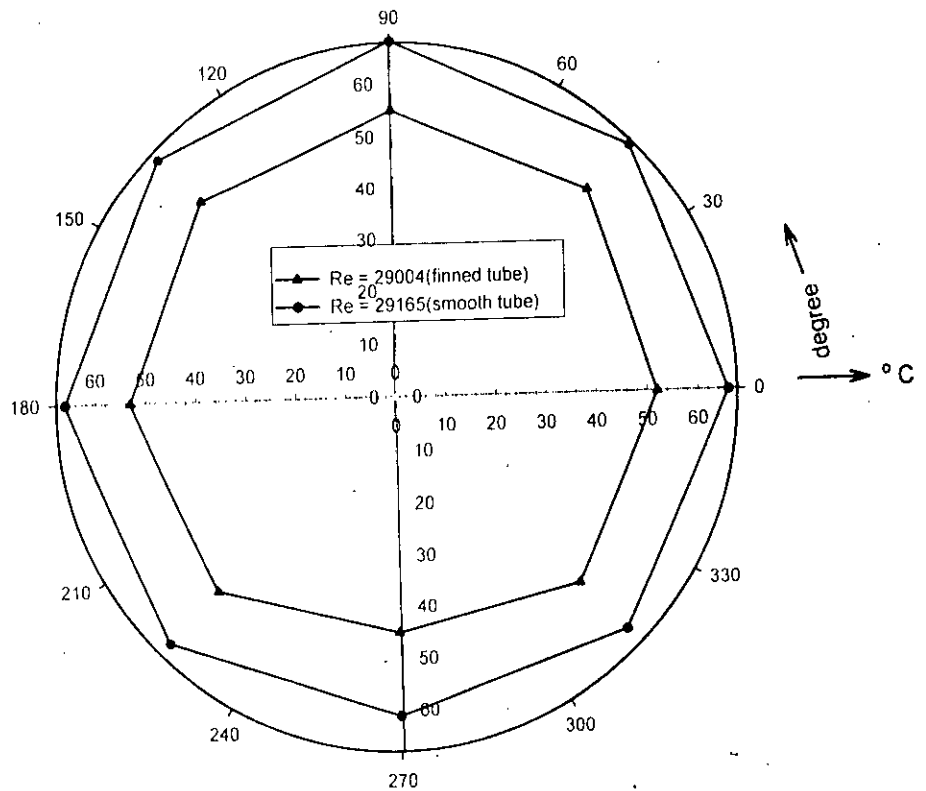
Figure 5.6: Radial temperature distribution around the outer surface of the test sections at insulated condituion
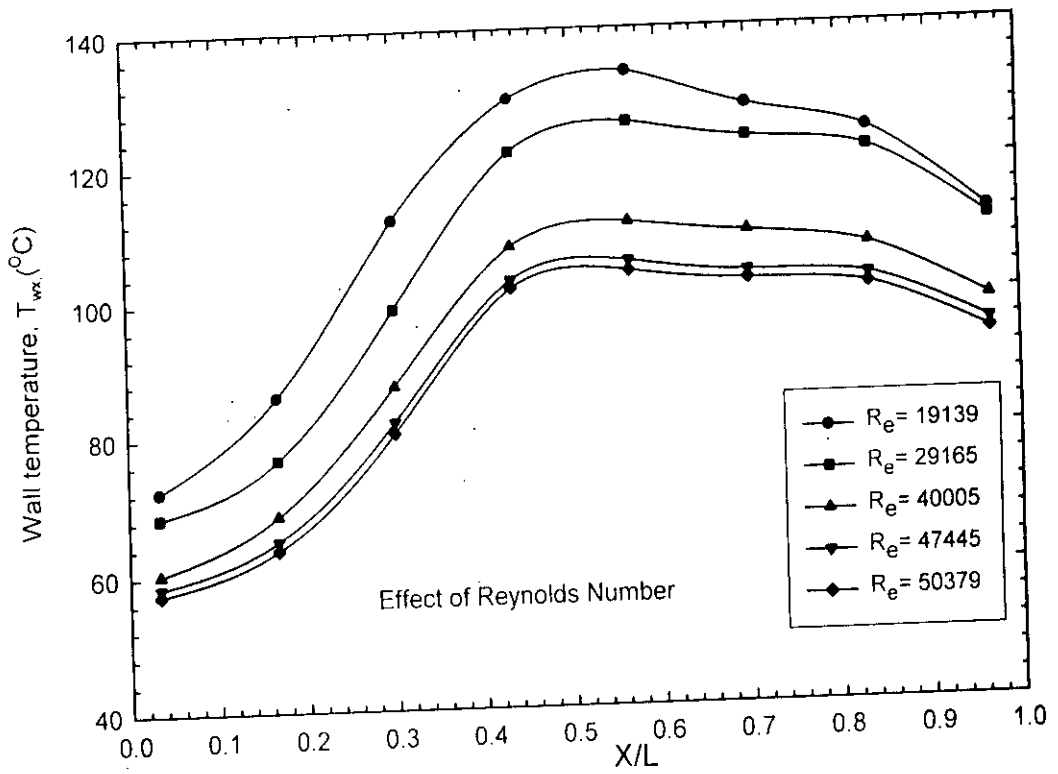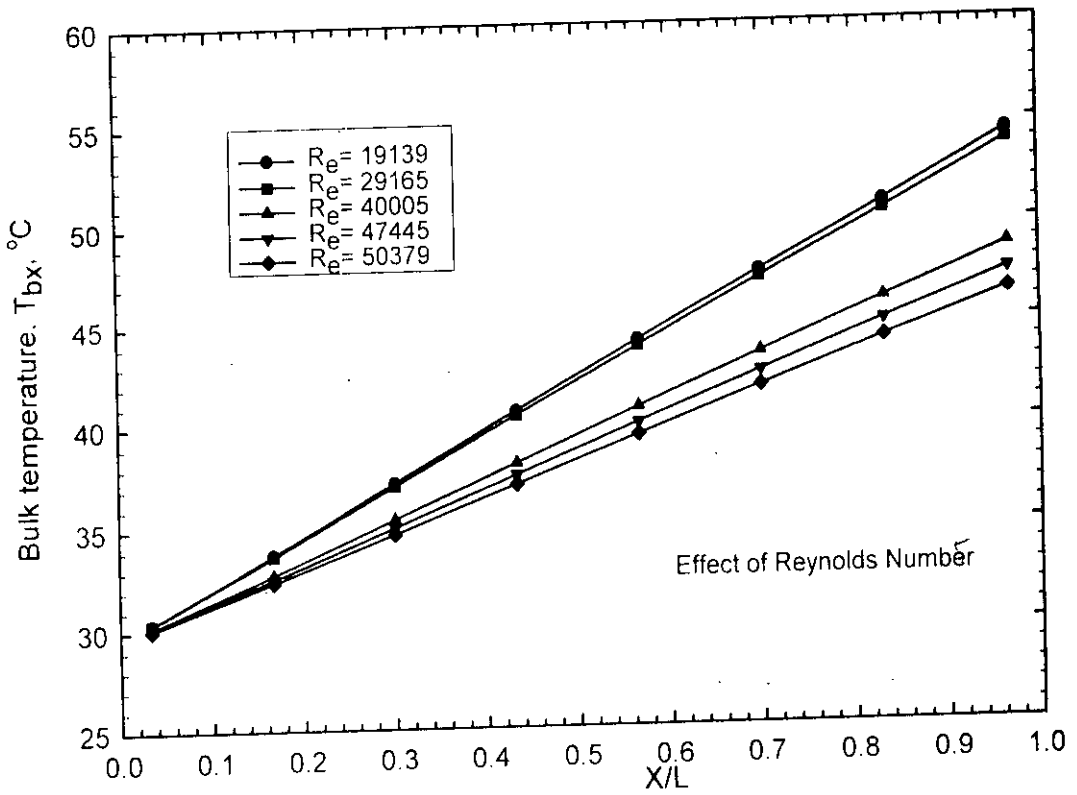
Figure 5.7: Bulk temperature distribution along the axial length of the smooth tube
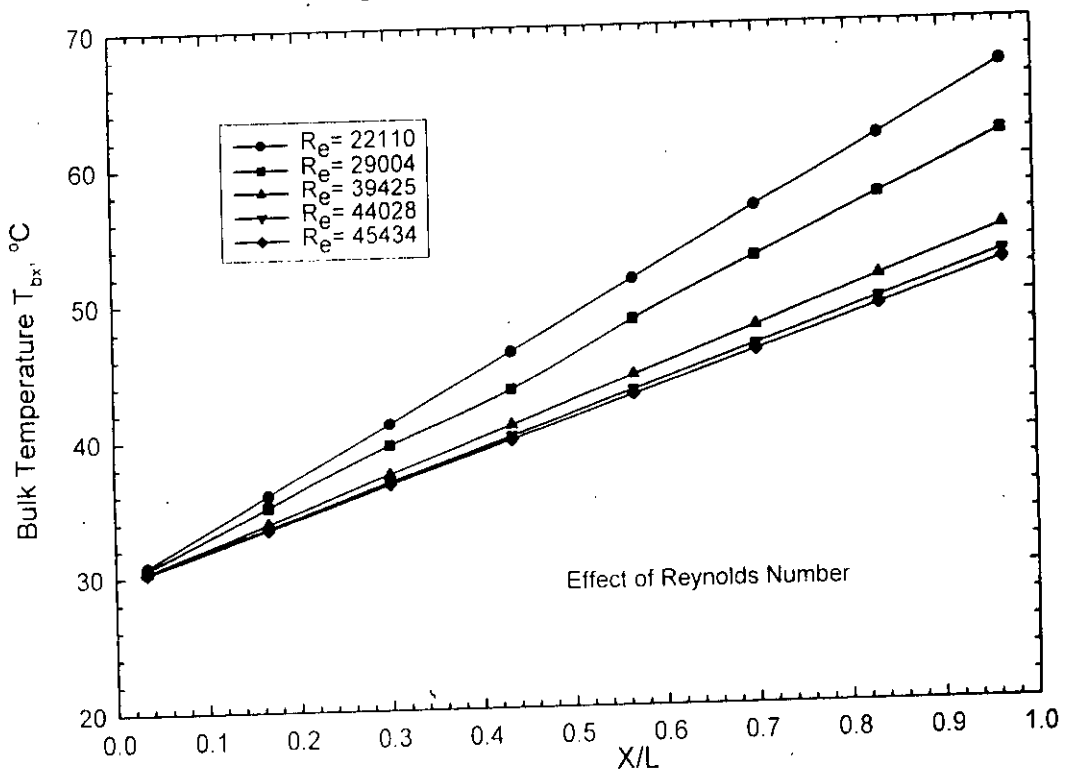
Figure 5.8: Bulk temperature distribution along the axial length of the finned tube
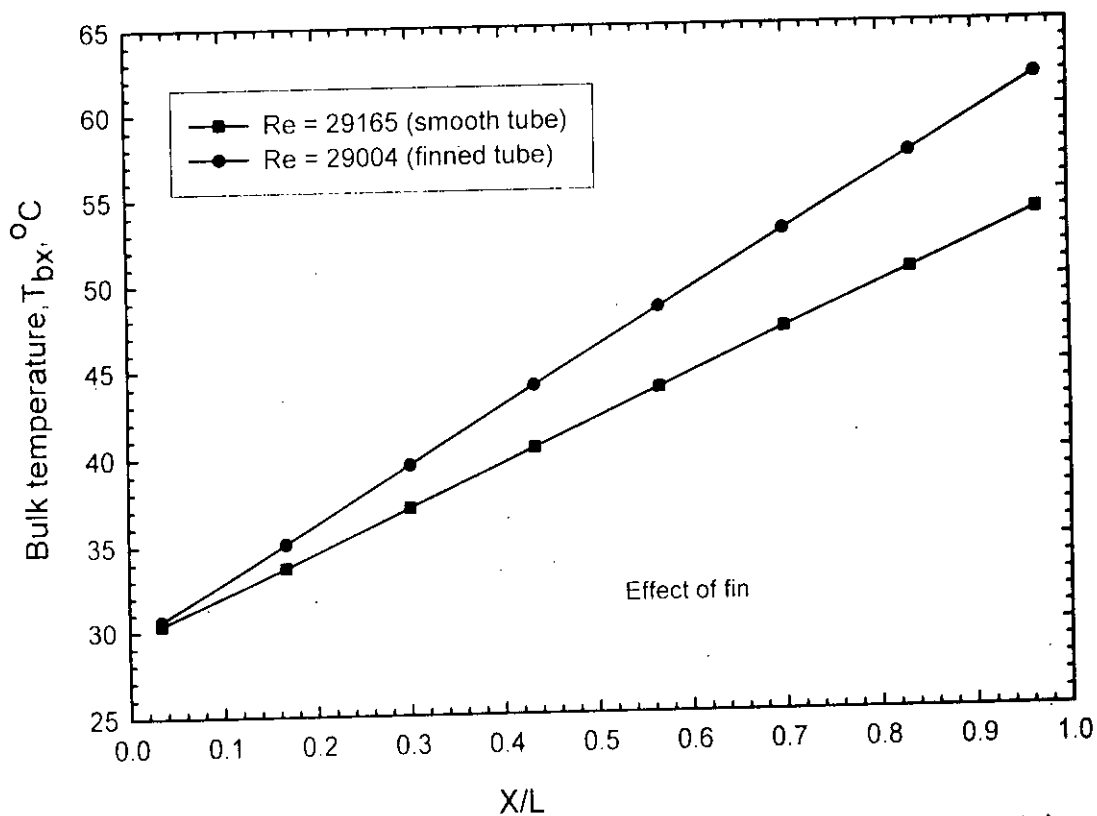
Figure 5.9 : Bulk temperature distribution along the length of the tube for compare able Reynolds number
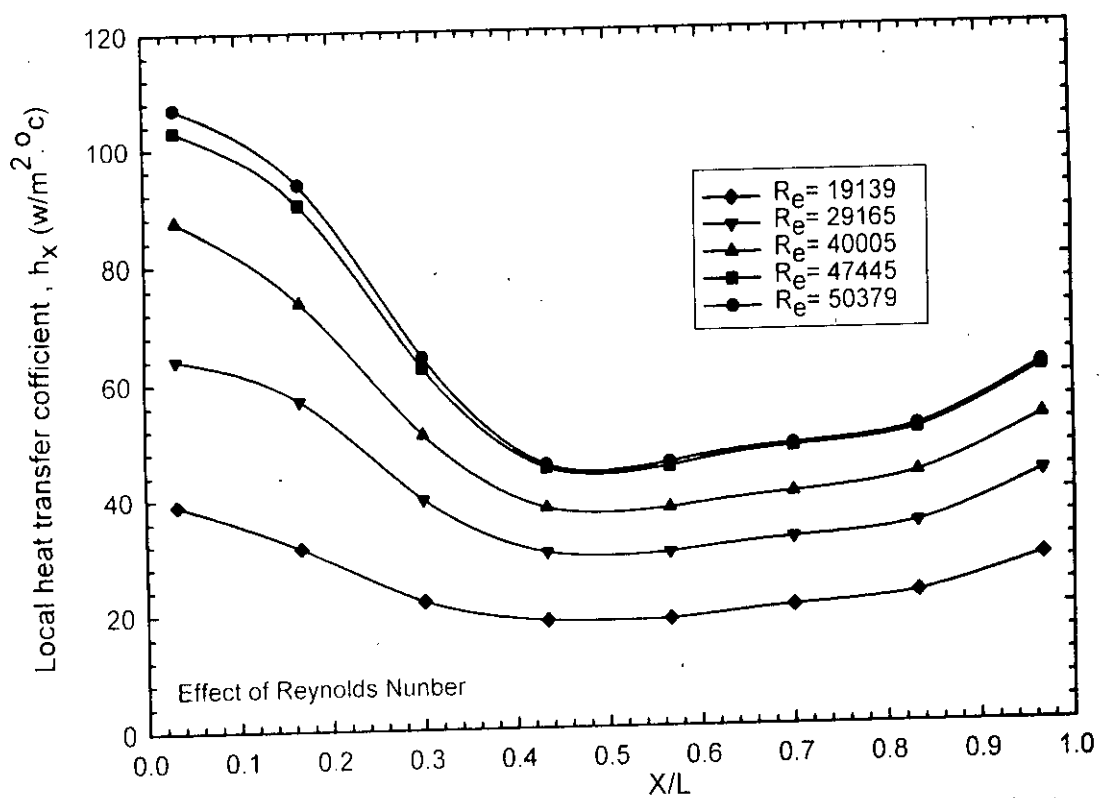
Figure 5.10: Longitudinal variation of local heat transfer cofficient of smooth tube
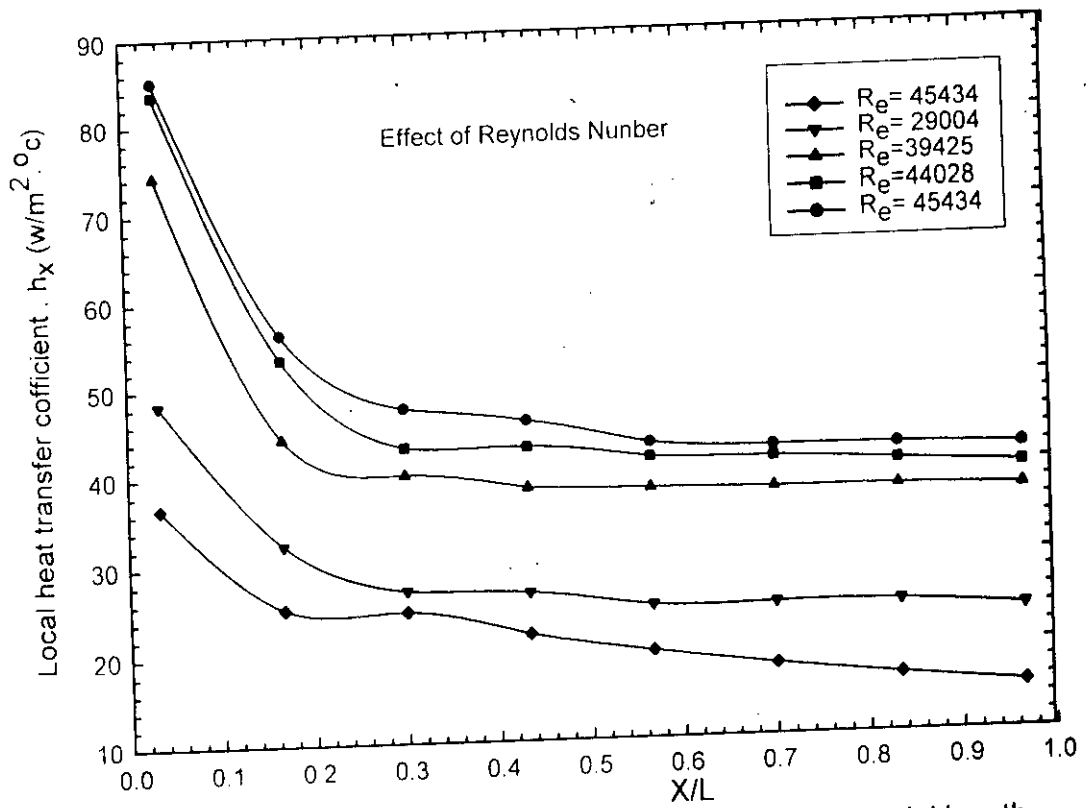
Figure 5.11: Local heat transfer cofficient along the axial length of the finned tube
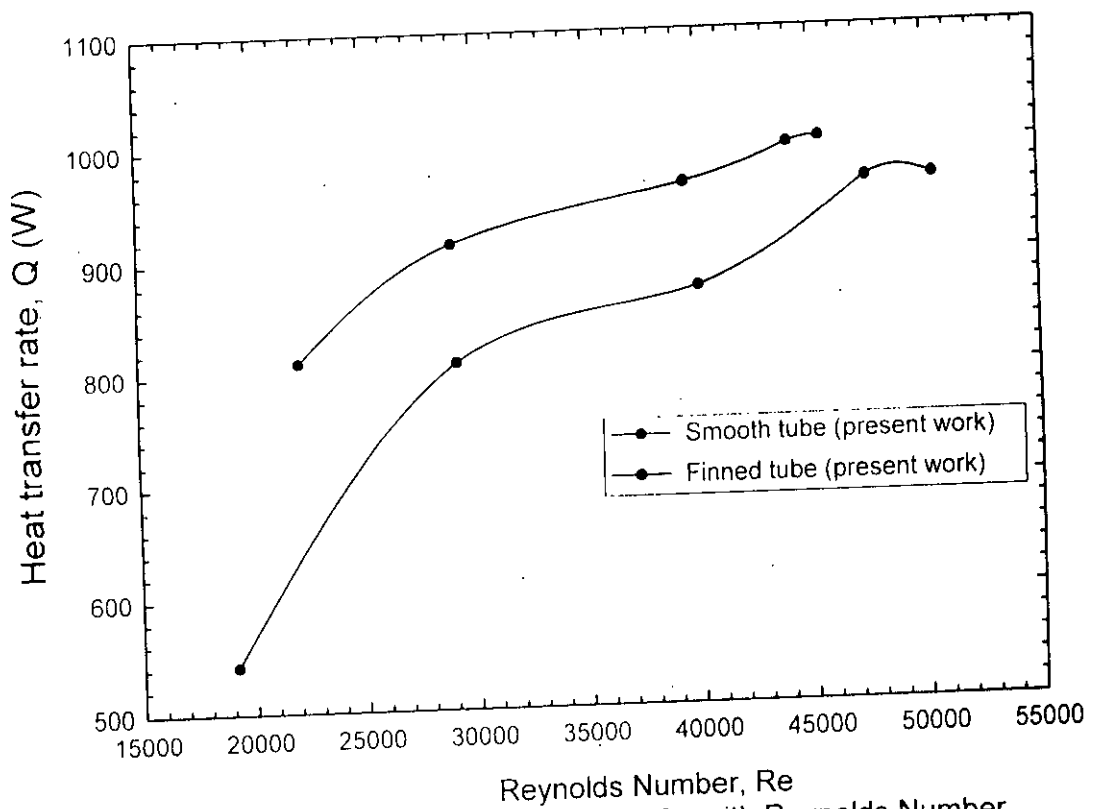
Figure 5.12: Variation of heat transfer with Reynolds Number
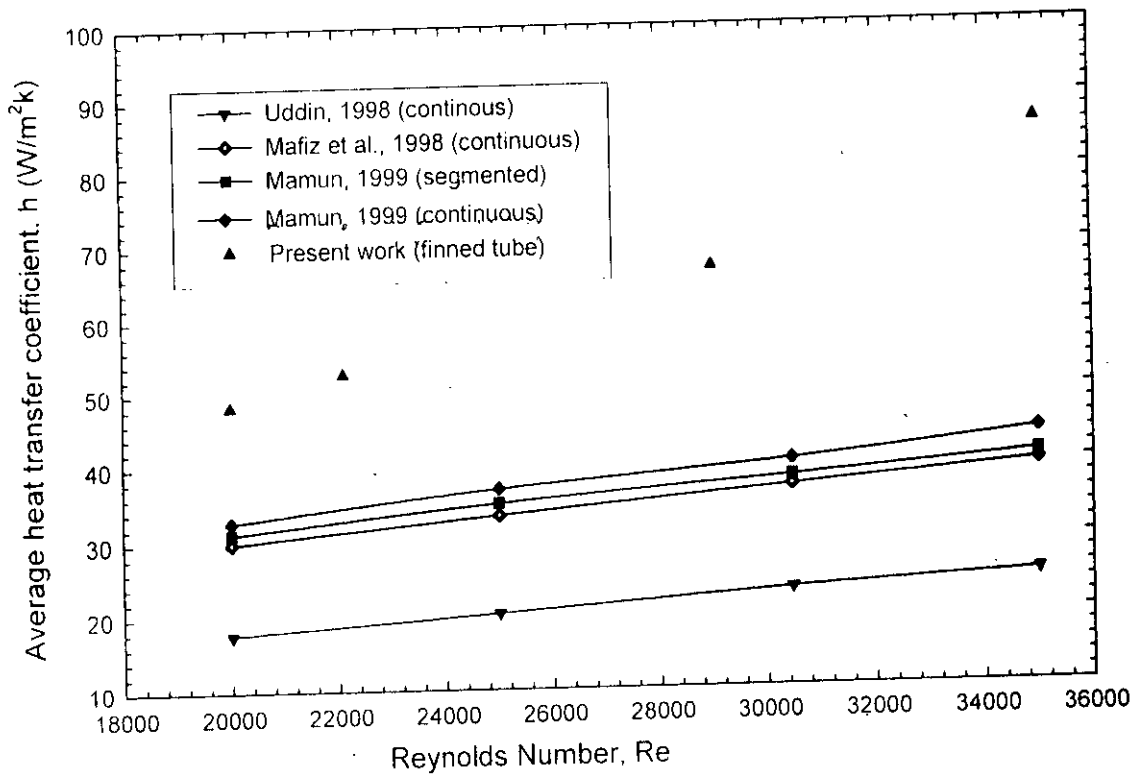
Figure 5.13: Comparison of average heat transfer coefficient for finned tube (based on D_i) with others experimental values.
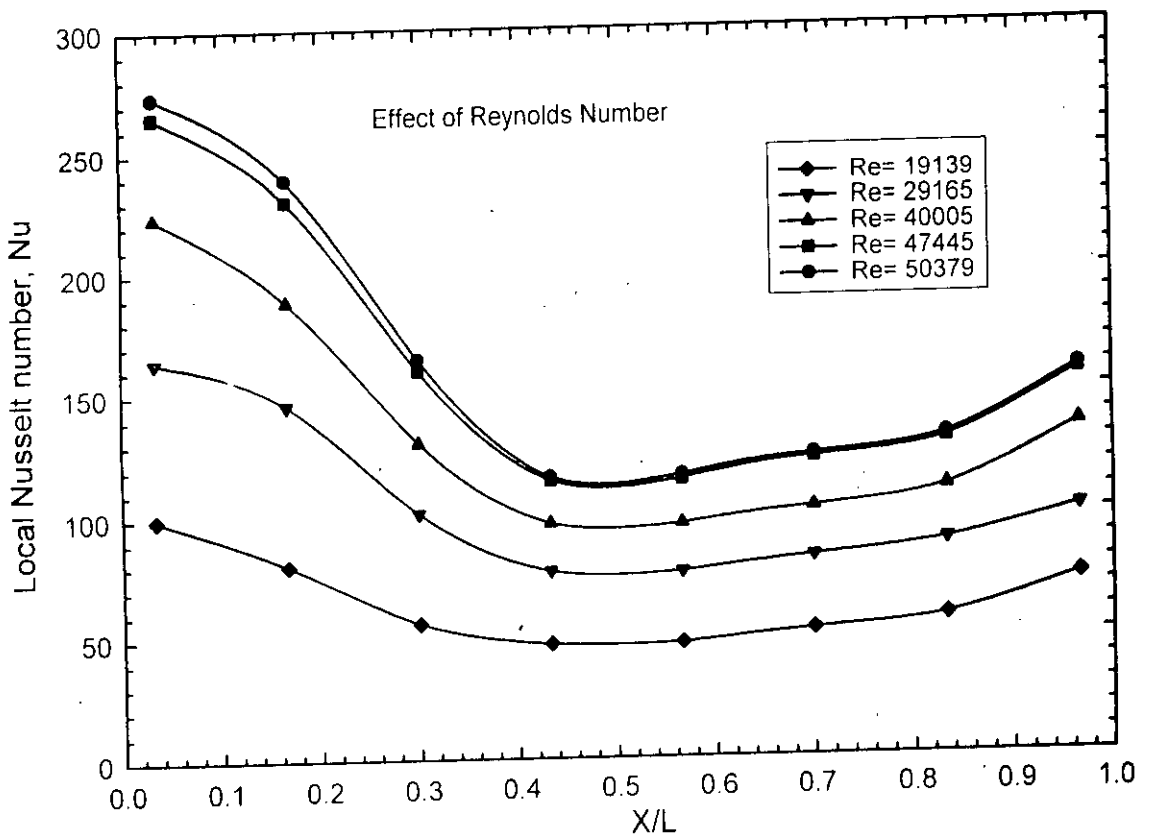
Figure 5.14: Local Nusselt number along the length of the smooth tube

41
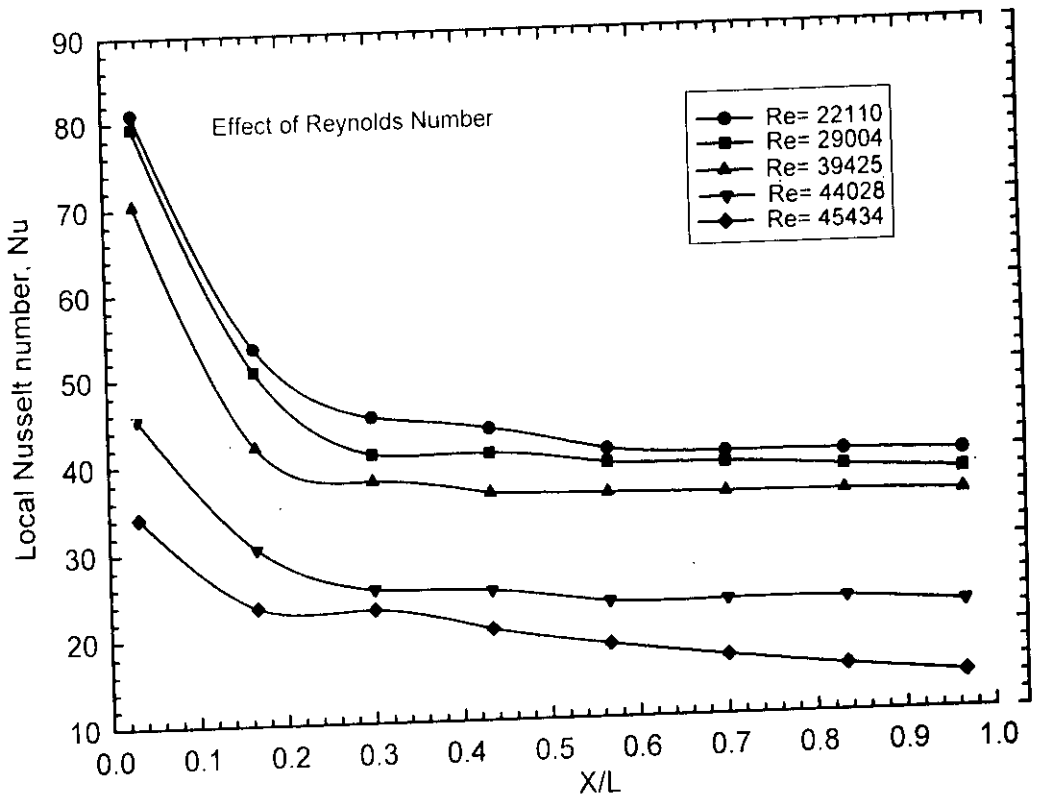
Figure 5.15 : Local Nusselt number along the length of the finned tube
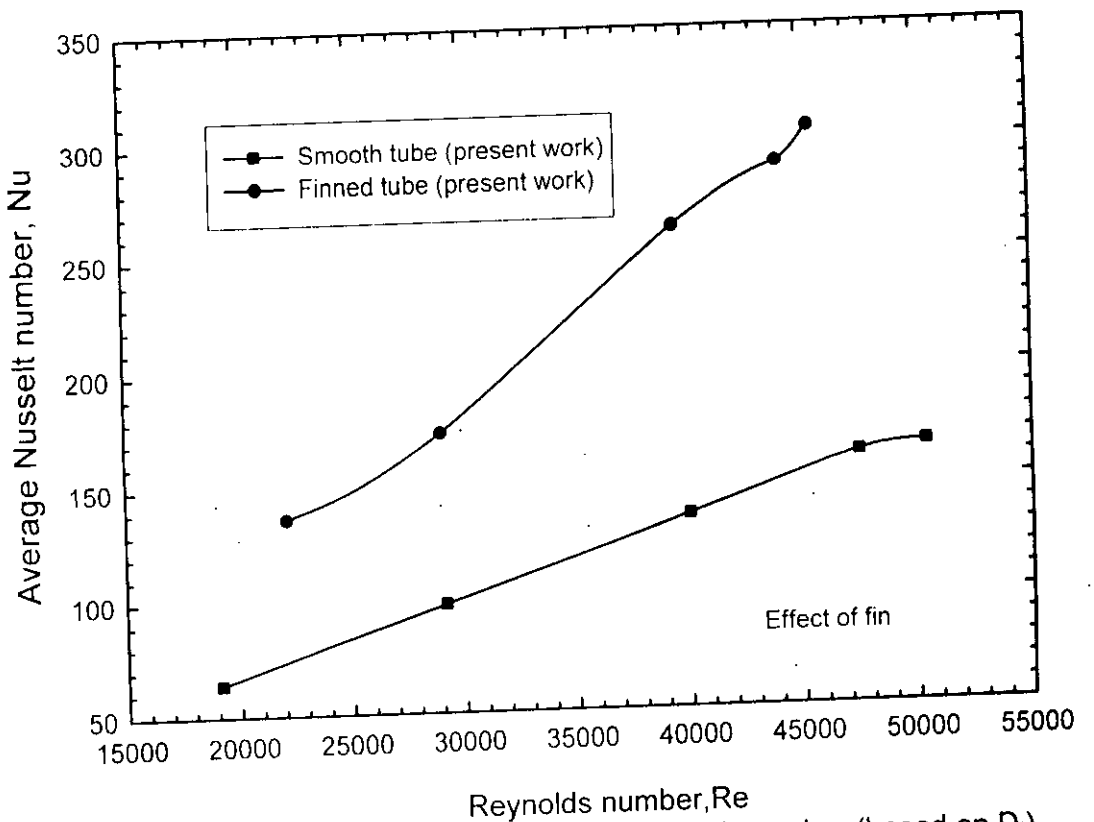
Figure 5.16: Comparism of average Nusselt number (based on D_i)
for both finned and smooth tube
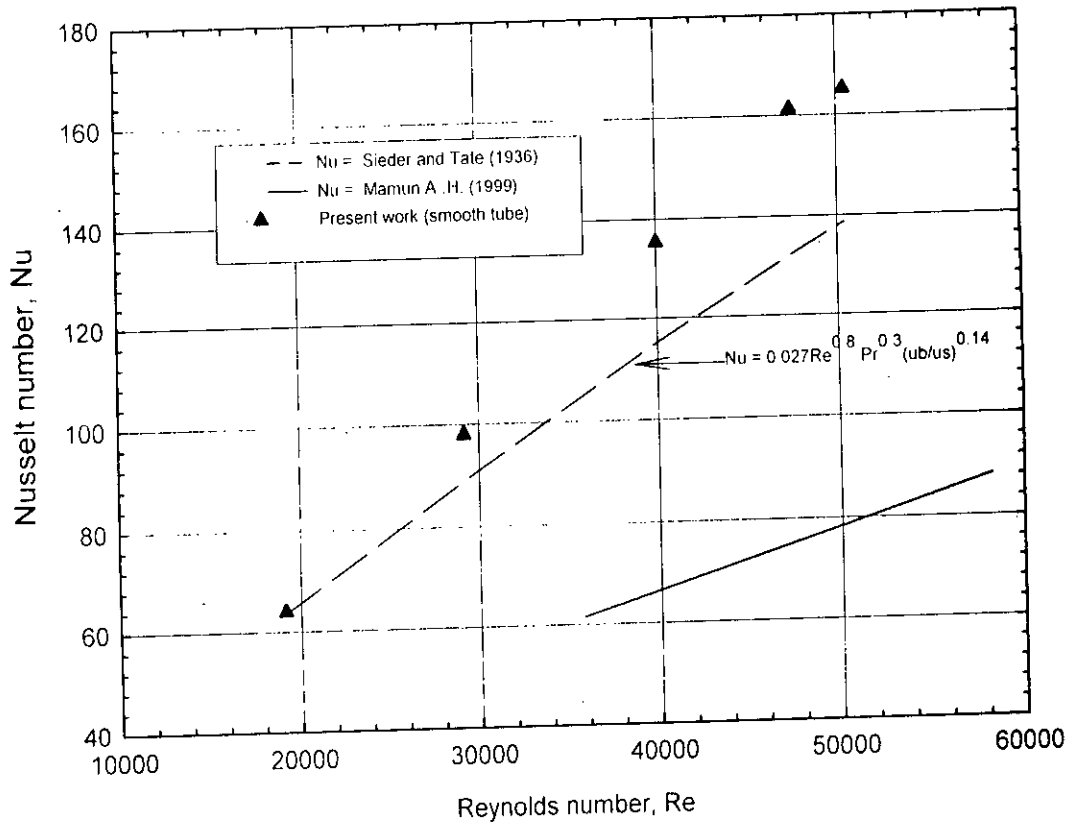
Figure 5.17: Comperisn of experimental data for smooth tube
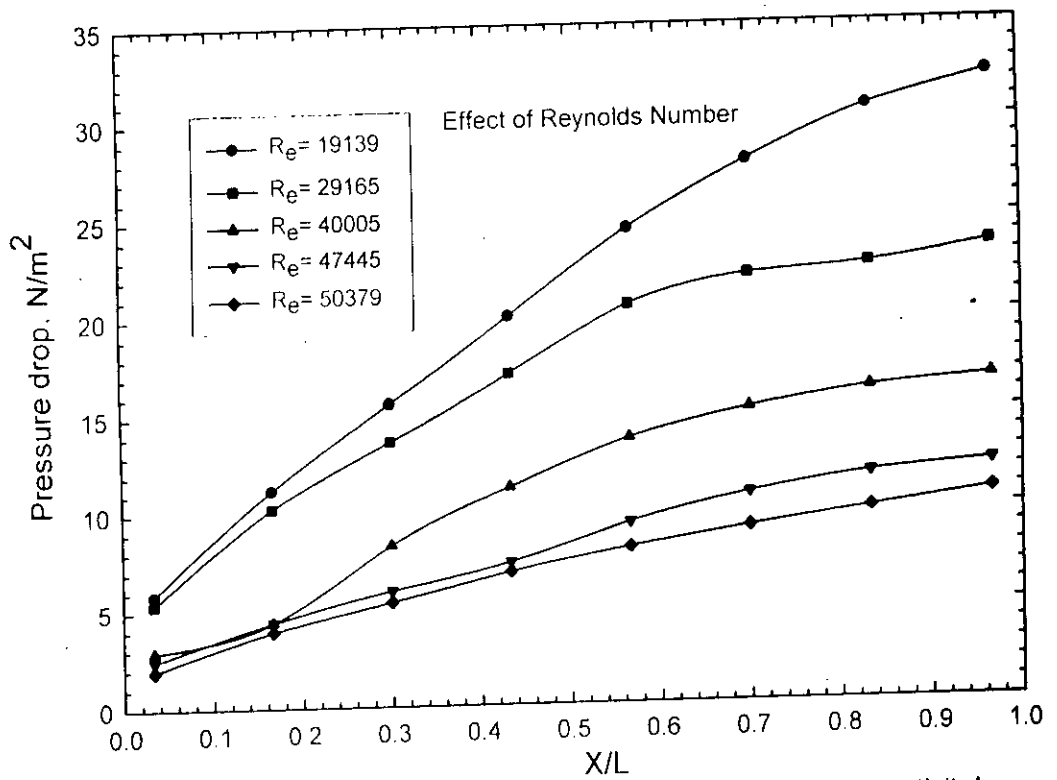
Figure 5.18: Pressure drop along the length of the smooth tube
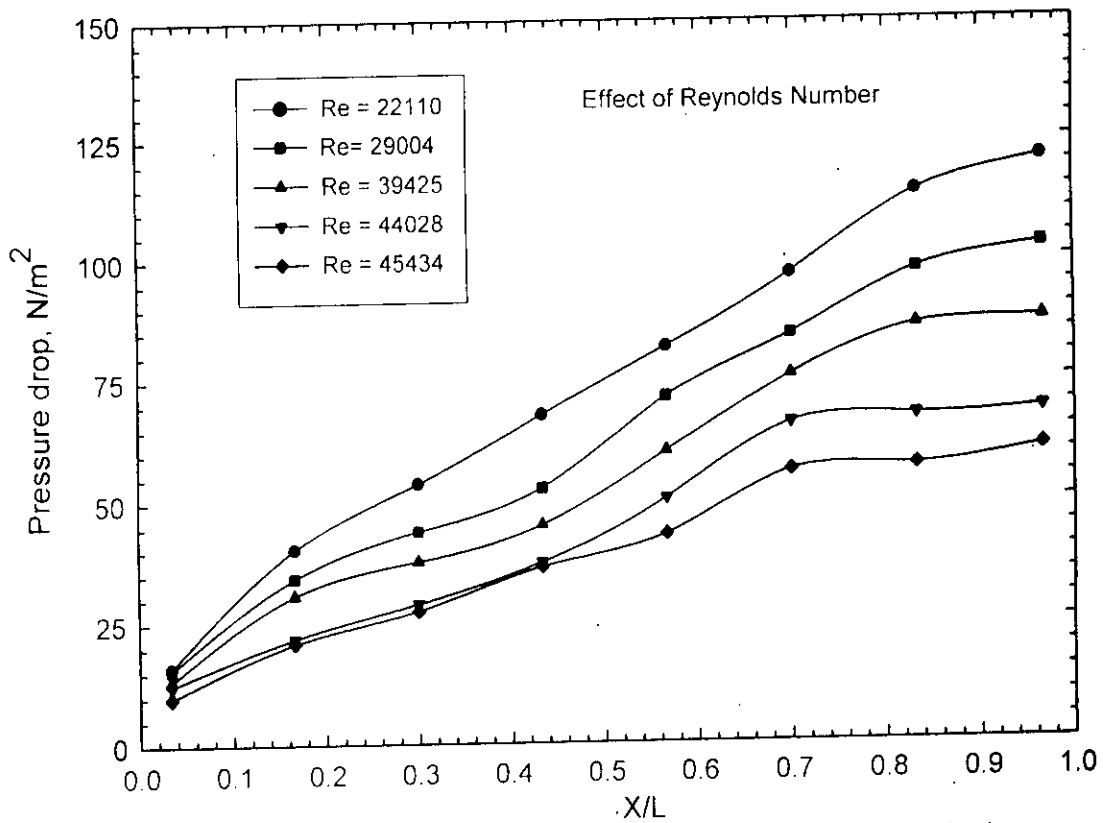
Figure 5.19: Pressure drop along the length of the finned tube
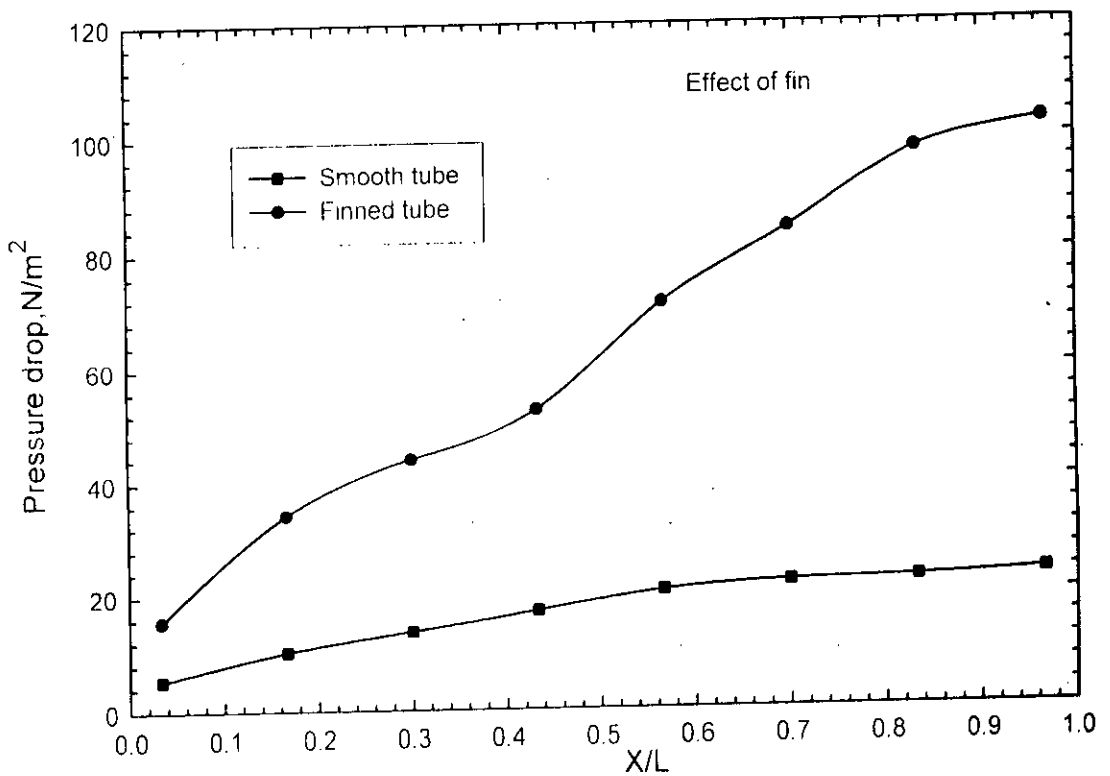
Figure 5.20: Pressure drop along the length of the tube
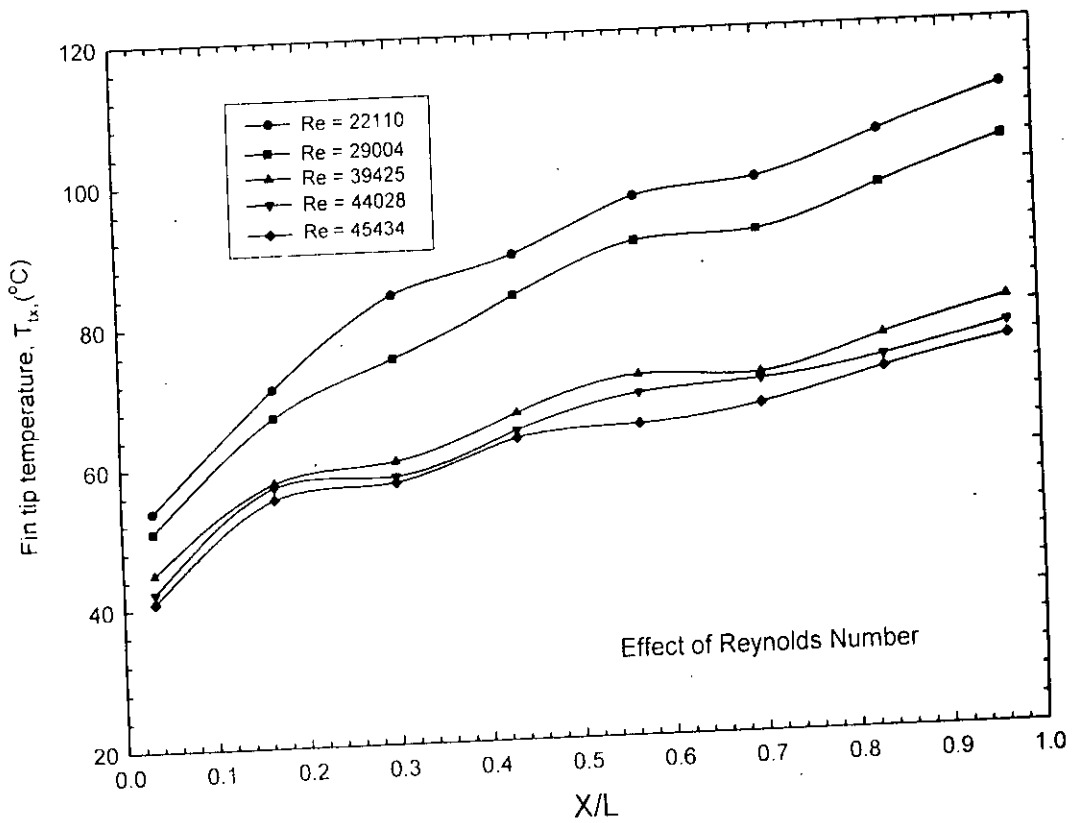for comparable Reynolds number
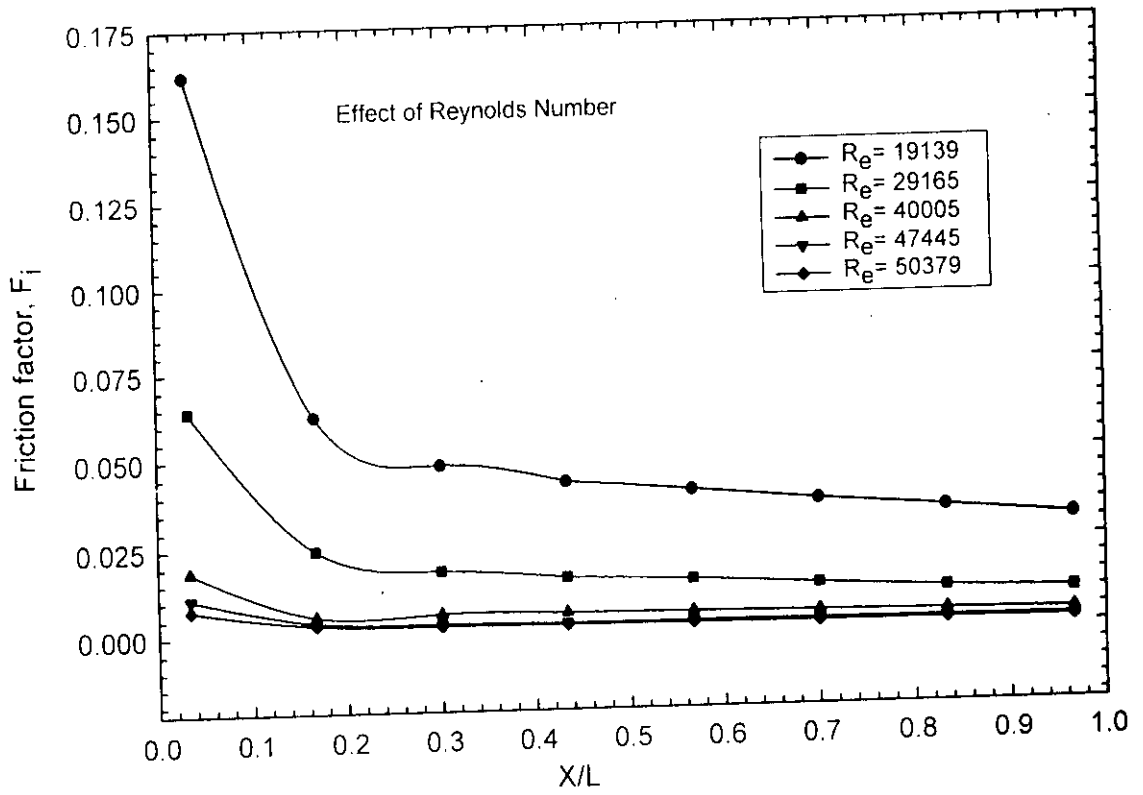
Figure 5.21: Friction factor along the axial length of the smooth tube
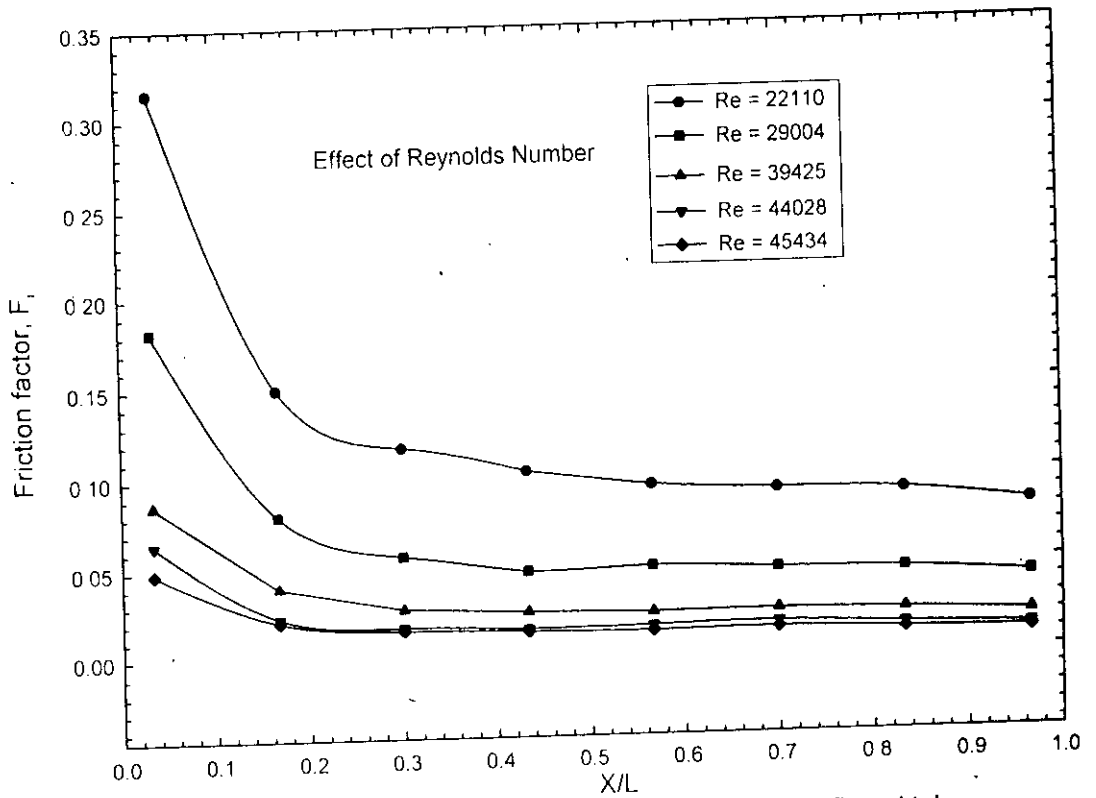
Figure 5.22: Friction factor along the length of the finned tube
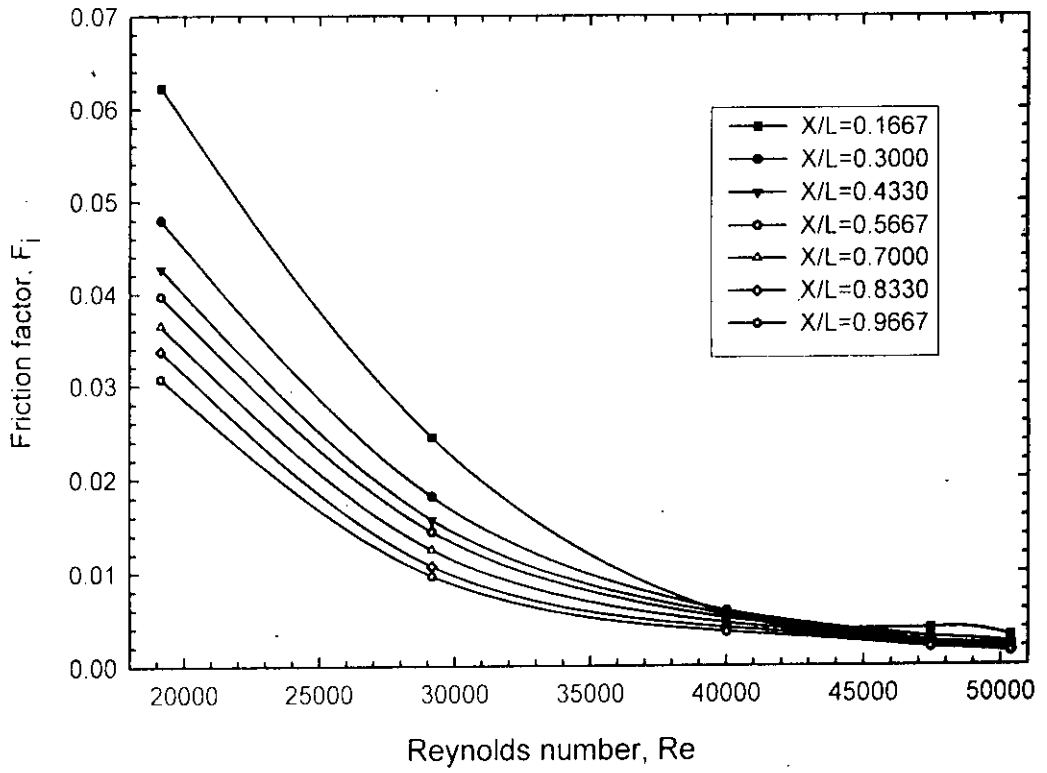
Figure 5.23: Variation of friction factor with Reynolds number for **smooth tube**
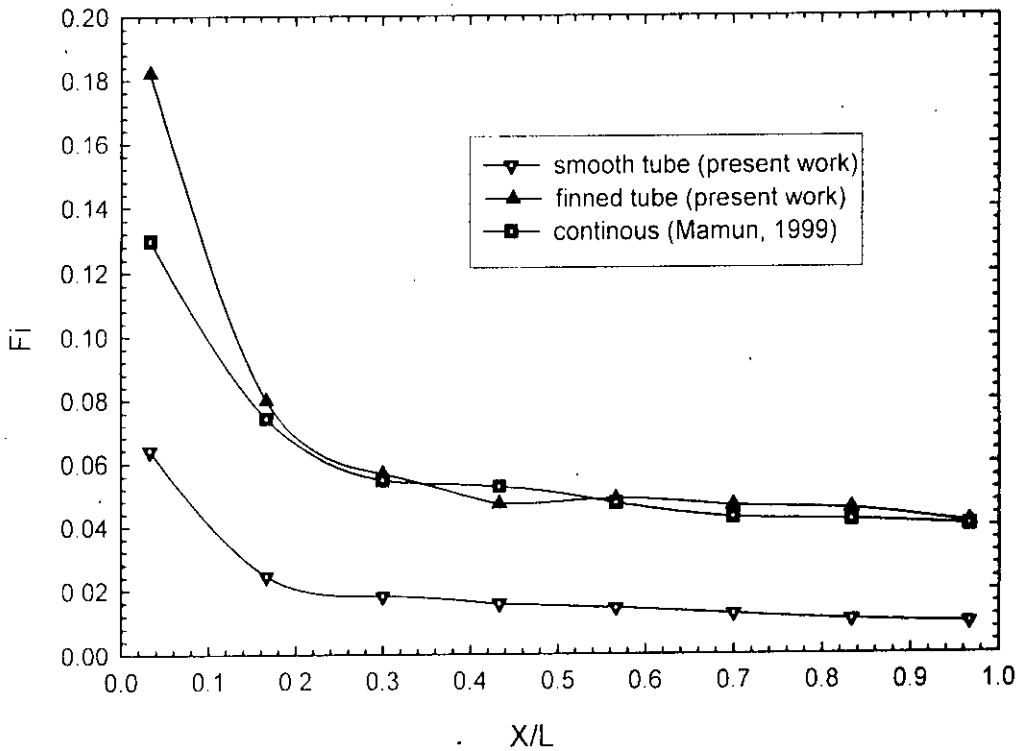
Figure 5.24: Comperison of friction factor for differenr test sections along the longitudinal direction of the tube for Re= 2.9×10^4.
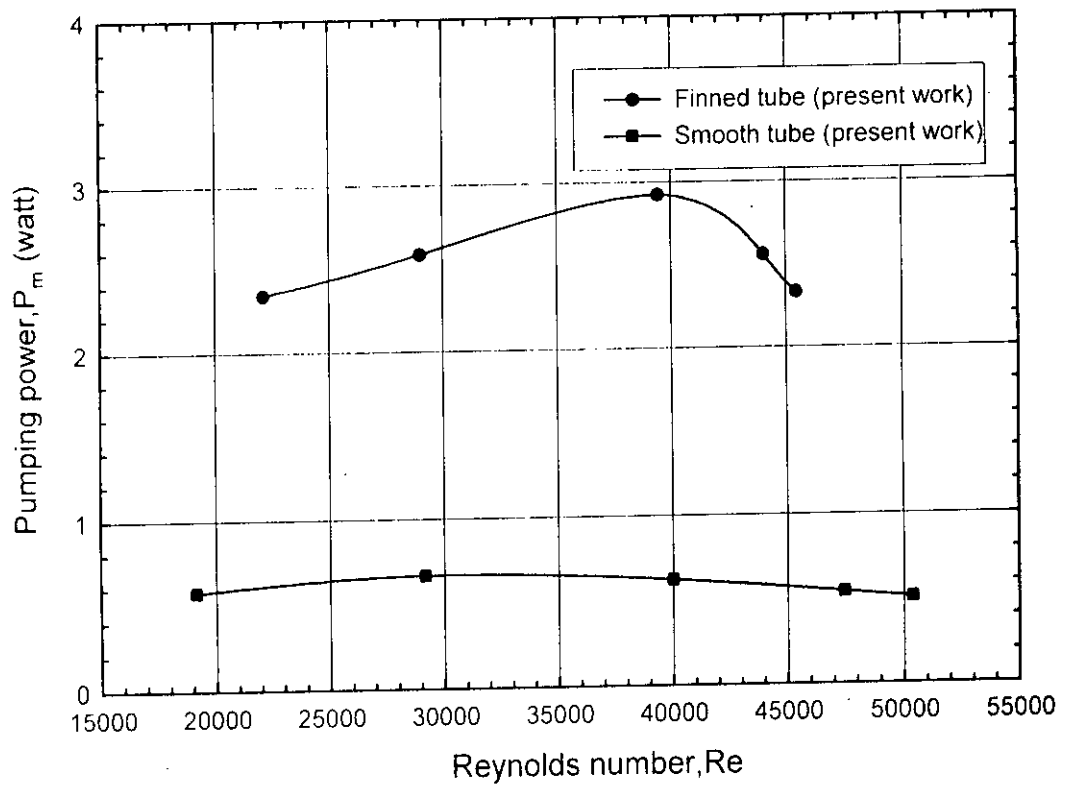
Figure 5.25: Comparism of pumping power with Reynolds number
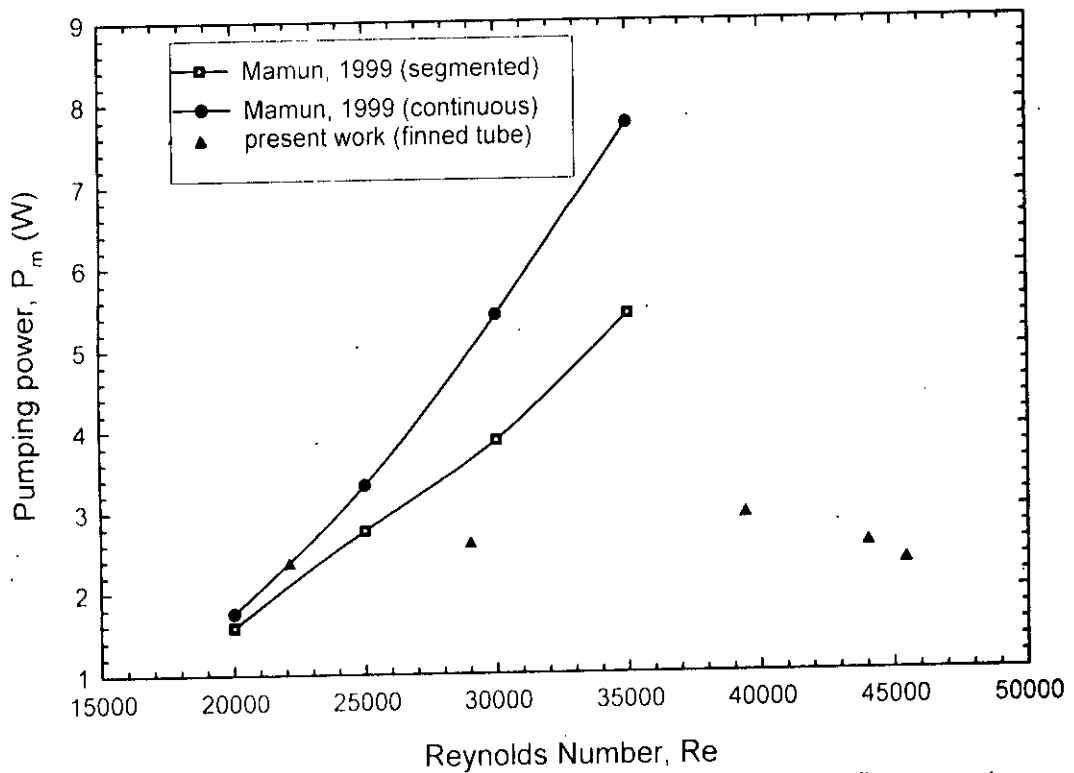
Figure 5.26: Comperison of pumping power for various fin geometry
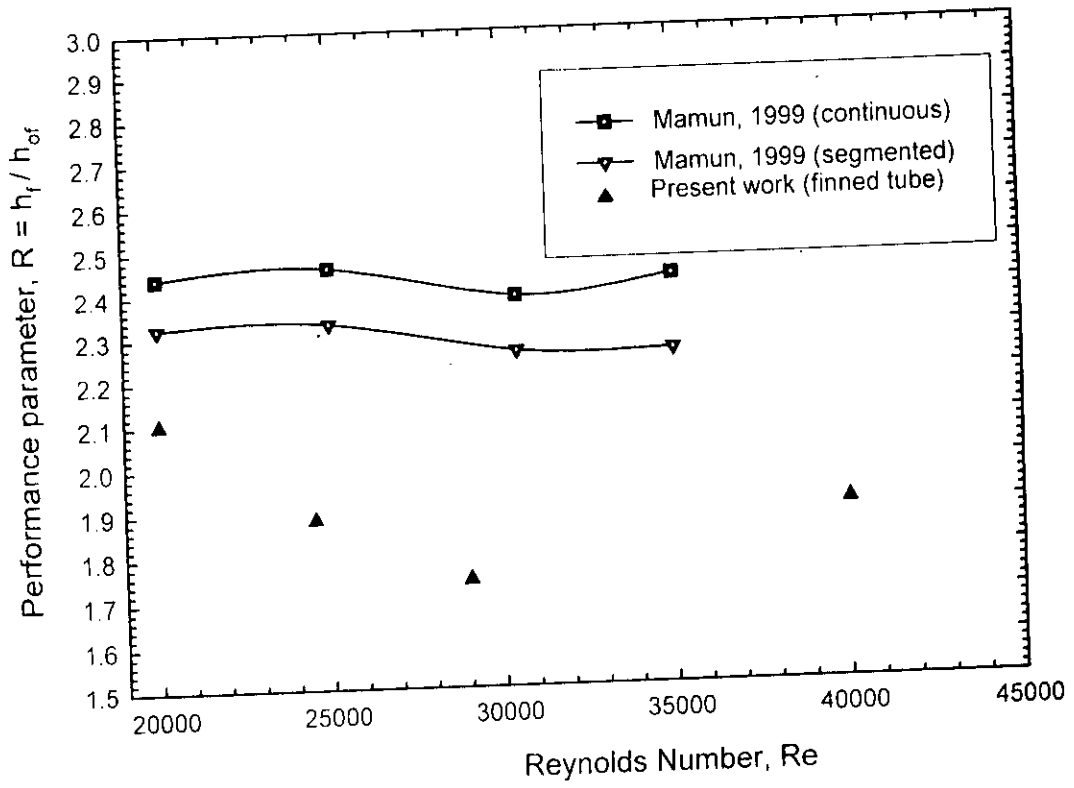
Figure 5.27: Comparison of performance parameter for different fin geometry.

6

CONCLUSIONS

Steady state fluid flow and heat transfer performance of a smooth tube as well as a tube having internal integral longitudinal T-section fins were studied experimentally. Results of the experiment are well presented and analyzed in the previous chapter. In this chapter summary of the analysis and some recommendations are enlisted.

6.1 CONCLUSIONS

In this article a quantitative comparison will be made for friction factor, heat transfer coefficient and pumping power for finned and smooth tube. All the findings are summarized below:

1. The friction factor of finned tube is about 3.0 to 4.0 times higher than that of smooth tube for Reynolds number range 2.0x104 to 5.0x10^4. But the slope of the friction factor of finned tube is very nearly equal to that of the smooth tube at every location of the test section.

2. The friction factor is high near the inlet section and drops gradually to the value corresponding to the fully developed flow.

3. Nusselt number is high in the entrance region and it decreases with increasing axial distance approaching asymptotically upto the corresponding value of fully developed flow.

4. The heat transfer coefficient for finned tube is about 1.5 to 2.0 times higher than that of smooth tube for the above mentioned Reynolds number range.

5. The pumping power of finned tube is about 3.5 to 4.5 times higher than that of smooth tube for those Reynolds numbers.

This experimental study has revealed that heat transfer coefficient of finned tube is large in the entrance region and the enhancement of heat transfer in the fully developed region is remarkable due to fin effects.

6.2 RECOMMENDATIONS

i. With some modifications of the experimental set up, the test section can be replaced by another one of varying tube diameter, number of fins, fin height, length of test section, working fluid, heating condition etc.

ii. The pitot tube can be replaced by a hot-wire anemometer for measurement of velocity at inlet section of the test piece.

REFERENCES

Bergles, A. E., Brown, J. S., and Snider, W. D., "Heat Transfer Performance of Internally Tubes," *ASME* paper No. 71, HT-31, American Society of Mechanical Engineers, New York, 1971.

Carnavos, T. C., "Heat Transfer Performance of Internally Finned Tubes in Turbulent Flow," *Heat Transfer Engineering Journal* Vol. 1 No. 4, pp. 32-37, 1980.

Chowdhury, D. and Patankar, S.V., "Analysis of Developing Laminar Flow and Heat Transfer in Tubes with Radial Internal Fins," Proc. *ASME National Heat Transfer Conference*, pp. 57-63, 1985.

Cox, R. B., G. A. Matta, A. S. Pascale, and K. G. Stromberg, "Second Report on Horizontal Tubes Multiple-effect Process Pilot Plant Tests and Design," Off Saline Water Res. Dev. Rep. No. 592 DSW, Washington, DC. May 1970.

Edwards, D. P. and Jensen, M. K., "Pressure Drop and Heat Transfer Predictions of Turbulent Flow in Longitudinal Finned Tubes," Advances in Enhanced Heat Transfer, *ASME HTD*-Vol. 287, pp. 17-23, 1994.

Fenner, G. W. and Ragi, E., "Enhanced Tube Inner surface Device and Method," U.S. pat. 4154, May 15, 1979.

Gee, D. L. and Webb, R. L., " Forced Convection Heat Transfer in Helically Rib-Roughed Tubes," International Journal of Heat and Mass Transfer Vol.23 pp. 1127-1136, 1980.

Goldstein L Jr. and Sparrow, E.M., "Experiments on the Transfer Characteristics of a Corrugated Fin and Tube Heat Exchanger Configuration,". J. Heat Transfer (98): 26-34, 1976.

Gunter, A. Y. and Shaw, W. A., "Heat Transfer, Pressure Drop and Fouling Rates of Liquids for Continuos and Noncontinuos Longitudinal Fires," Trans. ASME (64): 795-802, 1942.

Hiding, W. E. and Coogan, C. H., "Heat Transfer and Pressure Loss Measurements in Internal Finned Tubes," Symposium on Air Cooled Heat Exchangers, *ASME, National Heat Transfer Conference*, Clevelant, Ohio, pp. 57-85, 1964.

Kelkar, K. M. and Patankar, S. V., "Numerical Prediction of Fluid Flow and Heat Transfer in a Circular Tube with Longitudinal Fins Interrupted in the Streamwise Direction." Presented at the *National Heat Transfer Conference*, Pittsbrugh, Pensylvania, 1987.

Kern, D. Q. and Kraus, A. D., Extended Surface heat Transfer, McGraw-Hill, New York, 1972.

Kline, S. J.and McClintock, F. A., " Describing Uncertainties in Single-Sample Experiments," *Mechanical Engineering*, 75,Jan.,pp. 3-8, 1953.

Mafiz, H., Huq, A. M. A., and Rahman, "Experimental Measurements of Heat Transfer in an Internally Finned Tube". Accepted for publication in *the journal of International Communication in Heat and Mass Transfer*, CJ97/1890, 1998.

Mafiz, H., Huq, A. M. A., and Rahman, M. M., "An Experimental Study of Heat Transfer in an Internally Finned Tube," Proceedings *ASME* Heat Transfer Division, Volume-2, pp. 211-217, 1996.

Mamun, A. H. M., Md., "Pressure Drop and Heat Transfer In An Internally Finned Tube," Dept. of Mechanical Engg. *BUET*, Dhaka, 1999.

Nandakumar, K. and Masliyah, J. H., "Fully Developed Viscous Flow in Internally Finned Tubes," *Chemical Engineering Journal*, Vol. 10, pp. 113-120, 1975.

Ower, E and Pankhurst , R. C., "The Measurement of Air Flow.," Fifth Edition (in SI units), Pergamon Press, 1977.

Patankar, S. V. Ivanovic, M. and Sparrow, E. M., "Analysis of Turbulent flow and Heat Transfer in Internally Finned Tube and Annule." J. Heat Transfer (101): 29-37, 1979.

Prakash, C. and Liu, Y. D., "Analysis of Laminar Flow and Heat Transfer in the Entrance Region of an Internally Finned Circular Duct," Journal of Heat Transfer, Vol. 107, pp. 84-91, 1985.

Prakash, C. and Patankar, S. V., "Combined Free and Forced Convection in Vertical Tubes with Radial Internal Fins," Journal of Heat Transfer, Vol. 103, pp. 566-572, 1981.

Prince, W. J., "Enhanced Tubes for Horizontal Evaporator Desalination Process, "MS thesis in engineering, University of California, Los Angles, 1971.

Rustum, I. M. and Soliman, H. M.,"Numerical Analysis of Laminar Forced Convection in the Entrance Region of Tubes with Longitudinal Internal Fins," Journal of Heat Transfer, Vol. 110, pp. 310-313, 1988.

Shah, R. K, Mcdonald, C. F., and Howard, C. P., Compact Heat Exchangers-History, Technological Advancement and mechanical Design problems, HTD vol. 10, ASME, New York, 1980.

Shah, R. K., "Classification of Heat Exchangers", in Thermal-Hydraulic Fundamentals and Design. S.Kakac, A.E. Bergles, and F. Mayingers eds. Pp. 9-46, Hemisphere/McGraw-Hill, New York, 1980.

Sieder, E. N. and Tate, C. E., "Heat Transfer and Pressure Drop of Liquids in Tubes," Ind. Eng. Chem., vol. 28, p. 1429, 1936.

Uddin, J. M., "Study of Pressure Drop Characteristics and Heat Transfer Performance in an Internally Finned Tube," Dept. of Mech. Engg. BUET, Dhaka, 1998.

Watkinson, A. P., Miletti D. L., Kubanek, G. R., "Heat Transfer and Pressure Drop of Internally Finned Tubes in Laminar Oil Flow," ASME, American Society of Mechanical Engineers, New York, 1975.

Webb, R. L., "Air-Side Heat Transfer in Finned Tube Heat Exchangers," Heat Transfer Eng. Vol. 10, 33-49, 1980.

SPECIFICATION OF EQUIPMENT

1. **Fan:**

Capacity	:	30 m³/min.
Pressure	:	125 mm of water
H.P	:	3
Phase	:	3
Current	:	4.1 A
Voltage	:	380 V

2. **Temperature Controller:**

Range	:	0-200°C
Input voltage	:	220 V

3. **Electric Heating System:**

Heat Resistance	:	5.727 Ohm
Maximum Voltage	:	220 Volts
Maximum Current	:	25 A
Power	:	5.5 kW

4. **Data Acquisition System:**

Cole-Parmer (USA origin)

Number of inputs	:	14 Model PCA-14
Resolution	:	16 Bits
Accuracy	:	± 0.02% of range
Linearity	:	± 0.015 %
Input Impedance	:	10000 Megaohms/0.1 UF
Binary Inputs	:	11 ON-OFF TTL or Contact
Closure		or 10 – Bit pulse counter
Power	:	120 V 50/60 Hz 0.5 A

SAPMLE CALCULATIONS

For smooth tube:

Internal diameter of the tube, $D_i = 70$ mm

$$A_x = \frac{\pi D_i^2}{4} = \frac{\pi}{4}(0.07)^2 = 3.8485 \times 10^{-3} \text{ sq.m}$$

$$A_s = \pi D_i = \pi(0.07) = 0.2199 \text{ m}$$

Hydraulic Diameter:

$D_h = D_i = 0.07$ m

Determination of **Mean Velocity**, V:

$$\Delta P = \frac{1}{2}\rho V^2 \qquad \text{[From Bernoulli's equation]} \tag{B.1}$$

If v is m/s, ρ is Kg/m^3, Δp is N/m^2 and d is the velocity head expressed in cm of water, then-

$$\Delta p = \gamma_{water} \times d \tag{B.2}$$

$$= 9.81 \times 10^3 \times \frac{d}{10^2} = 98.1 \times d \quad N/m^2$$

Standard atmospheric properties at the sea level are pressure = 760 mm of Hg

Temperature = $15^\circ C$

Density = $1.225 \ Kg/m^3$

For any other temperature, t $^\circ C$ and pressure, b mm of Hg, the value of the velocity in Kg/m^3 can be calculated as-

$$\rho_2 = \frac{P_2}{P_1} \cdot \frac{T_2}{T_1} \cdot \rho_1 = \frac{b}{760} \times \frac{(273+15)}{(273+t)} \times 1.225 \tag{B.3}$$

From equation (B-1), (B-2) and (B-3)

$$\frac{1}{2} \times \frac{b}{760} \times \frac{(273+15)}{(273+t)} \times 1.225 \times V^2 = 98.1 \times d$$

$$\Rightarrow V = 20.558\sqrt{\frac{273+t}{b}} \cdot \sqrt{d}$$

$$\Rightarrow V = C\sqrt{d} \qquad\qquad\qquad\qquad\qquad\qquad (B.4)$$

where, $C = 20.558\sqrt{\dfrac{273+t}{b}}$

Room condition:

Temperature, $t = 29.5°C$

Pressure, $b = 741.5$ mm of Hg

$$\therefore C = 20.558\sqrt{\frac{273+29.5}{741.5}} = 13.131$$

The experiment was conducted using a manometric fluid of sp. gr = 0.855 but it was recommended to perform with a fluid of sp. gr = 0.834. For this reason a correction is need which is as follows:

$\omega d = \omega_1 d_1$

$\Rightarrow 0.834\, d = 0.855\, d_1$

$\Rightarrow d = 1.0252\, d_1 = 0.855 \times 1.0252 \times d_1 = 0.8765\, d_1$

$\Rightarrow d = 0.8765 \times 2.54\, d_1$ cm   [d_1 is in inch of water]

$\Rightarrow d = 2.2263\, d_1$ cm

Measurement of mean velocity of 11 points is as follows:

Mean velocity, $V_i = \dfrac{\left(\sqrt{d_1} + \sqrt{d_2} + \sqrt{d_3} + \ldots\ldots + \sqrt{d_{11}}\right)}{11}$

$\qquad\qquad = 7.0878$ m/s

Mass flow rate, $M = \rho A_x V_i$

$\qquad\qquad = 1.1684 \times 3.8485 \times 10^{-3} \times 7.0878 \qquad \left[\begin{array}{c}\rho \text{ of air at 302.5k (room temp.)}\\ = 1.1684\, kg/m^3\end{array}\right]$

$\qquad\qquad = 0.031871$ kg/s

Reynolds Number:

$Re = \dfrac{\rho V\, D_i}{\mu} = 29165.68$, where $V = \dfrac{M}{\rho_b A_x}$, $\left[\begin{array}{c}\text{Properties of fluid are calculated}\\ \text{at its fluid bulk temp.}\end{array}\right]$

Friction Factor:

Local friction factor based on inside diameter is given by

$$F_i = \frac{(-\Delta P/x)D_i}{2\rho V^2} \qquad [\text{where } \Delta P \text{ is in N/m}^2]$$

(B.5)

$$= 5.96285 \times 10^{-4}(-\Delta P/x)$$

[ρ of water at 29.5°C (room temp.) is 995.84 kg/m^3]

Table B.1   Experimental data of fluid flow of smooth tube

Axial distance, x(mm)	Tapping pressure (mm of water)	Tapping pressure (N/m^2)	Pressure drop,ΔP (N/m^2)	F_i
0.0	5.6			
50	6.15	58.615	5.37	0.064
250	6.65	60.569	10.26	.02445
450	7.0	66.430	13.68	0.0181
650	7.35	73.269	17.1	0.0157
850	7.70	74.246	20.52	0.0144
1050	7.85	75.711	21.98	0.0125
1250	7.0	77.177	22.47	0.0107
1450	8.0	78.154	23.45	0.0097

Heat transfer calculation:

Air inlet temperature (room temperature), $T_i = 29.5$°C

Air outlet temperature, $T_o = 54.71$°C

Properties of air are calculated at fluid bulk temperature as-

C_p =   1.00669 kJ/Kg.°C

K   =   0.02738 W/m.k

μ =   2.018 x 10^{-5} kg/m.s

ρ =   1.1232 kg/m^3

Total heat taken by air, Q   = $MC_p(T_o - T_i)$

    =   0.031871 x 1.00669 x 10^3 (54.71-29.5)   W

    =   808.843   W

Heat taken of per unit area , $Q' = \dfrac{Q}{A_s L}$

$$= \frac{808.843}{0.2199 \times 1.5}$$

$$= 2452.154 \ W/m^2$$

The local bulk temperature of the fluid can be calculated according to the following way-

$$Q' = \frac{Q}{A_s L} = \frac{MCp(\Delta T)}{A_s L}$$

$$\Rightarrow \Delta T = \frac{Q' A_s L}{MCp}$$

Now, bulk temperature,

$$T_{bx} = T_i + (\Delta T)_x$$

$$= T_i + \frac{Q' A_s \cdot x}{MCp}$$

$$= 29.5 + \frac{2452.154 \times (0.2199)x}{0.031871 \times 1.00669 \times 10^3}$$

$$= 29.5 + 16.8066x \ {}^0C \tag{B.6}$$

Local convective heat transfer co-efficient is given by

$$h_x = \frac{Q'}{(T_w - T_b)x} = \frac{2452.154}{(T_w - T_b)x} \qquad W/m^2 \ {}^0C$$

Local Nusselt Number is, $N_{ux} = \dfrac{h_x D_h}{K}$

$$= \frac{0.07 h_x}{0.02738} = 2.5566 h_x$$

Table B.2 Experimental data of heat transfer of smooth tube

X (m)	T_{bx} (°C)	T_{wx} (°C)	h_x (w/m^2.°C)	N_{ux}
0.05	30.34	68.59	64.109	163.901
0.25	33.70	76.71	57.014	145.762
0.45	37.06	98.83	39.698	101.492
0.65	40.42	121.77	30.143	77.064
0.85	43.76	125.94	29.8388	76.286
1.05	47.15	123.43	32.147	82.187
1.25	50.51	121.53	34.528	88.274
1.45	53.87	110.77	43.096	110.179

Average heat transfer coefficient,

$$\bar{h} = \frac{Q}{A(T_{wav} - T_{bav})}$$

$$= \frac{Q'}{(T_{wav} - T_{bav})}$$

$$= \frac{2452.154}{T_{wav} - T_{bav}}$$

$$= \frac{2452.154}{106.01 - 42.05625}$$

$$= 38.3426 \quad W/m^2 .^{\circ}C$$

Average Nusselt number,

$$N_u = 2.5566 \, \bar{h}$$

$$= 98.0267$$

Pumping Power, $P_m = \frac{\Delta P}{\rho} . M = 0.6396 \, W$

For Finned Tube:

Hydraulic diameter, $D_h = \frac{4 \times A_{xf}}{W_{ft}}$

Here, wetted perimeter of finned tube, $W_{ft} = \pi D_i - 6 \times w + 6 \times w_f$

$$= 531.91 \, mm$$

$$= 0.53191 \, m$$

Cross sectional area of the finned tube, $A_{xf} = \frac{\pi}{4} D_i^2 - 6 \times A_f$

$$= 3362.451 \, mm^2$$

$$= 3.362 \times 10^{-3} \, m^2$$

$\therefore$ Hydraulic diameter, $D_h = \frac{4 \times 3.362 \times 10^{-3}}{0.53191}$

$$= 0.025282 \, m$$

Mean velocity at inlet section, $V_i = \frac{\left(\sqrt{d_1} + \sqrt{d_2} + \sqrt{d_3} + ... + \sqrt{d_{11}}\right)}{11}$

$$= 6.2049 \, m/s$$

Mass flow rate, $M = \rho A_x V_i$

$$= 0.026979 \, kg/s$$

[Properties of air are calculated at room temperature 29.5°C; $\rho = 1.1298 \, Kg/m^3$]

Mean velocity inside test section, $V = \dfrac{M}{\rho A_{xf}} = 7.491 \text{ m/s}$

[ρ at fluid bulk temperature 46.205°C = 1.0712 kg/m³]

and $\mu = 19.366236 \times 10^{-6}$ N.s/m²

Reynolds Number based on inside diameter, $Re = \dfrac{\rho V D_i}{\mu} = 29004.35$

Friction Factor

Local friction factor based on inside diameter may be given by

$$F_i = \frac{(\Delta p/x)D_i}{2\rho V^2} = 5.822612471 \times 10^{-4} \times (\Delta p/x) \qquad (B-7)$$

[ρ of air is at fluid bulk temperature and that of water at 29.5°C (room temperature) is 995.84 Kg/m³]

Table B.3   Experimental data of fluid flow of finned tube

Axial distance x (mm)	Tapping pressure (mm of water)	Tapping pressure (N/m²)	Pressure drop, ΔP (N/m²)	F_i
0.0	4.0	39.076		
50	5.6	54.707	15.631	0.1788
250	7.5	73.36	34.285	0.0705
450	8.5	83.04	43.964	0.0568
650	9.4	91.74	52.66	0.0525
850	11.3	110.39	71.314	0.0488
1050	12.6	123.09	84.014	0.0466
1250	14	136.77	97.69	0.0451
1450	14.5	141.65	102.58	0.0439

Heat transfer Calculation:

$T_i = 29.5°C$

$T_0 = 62.91°C$

Properties of air are calculated at fluid bulk temperature of 46.205°C.

C_p = 1014.93 J/Kg K

K = 0.02693 W/mk

μ = 19.3662 x 10^{-6} N.s/m^2

ρ = 1.0712 Kg/m^3

Total heat taken by air, $Q = MC_p(T_o - T_i)$

$$= 914.826 \text{ W}$$

Local heat transfer per unit area, $Q' = \dfrac{Q}{w_{ft} \times L}$

$$= \dfrac{914.826}{0.53191 \times 1.5}$$

$$= 1146.592 \quad W/m^2$$

The local bulk temperature of fluid can be calculated according to the following way

$$Q' = \dfrac{Q}{w_{ft} \times L}$$

$$= \dfrac{MC_p(\Delta T)}{w_{ft} \times L}$$

$$\Rightarrow \Delta T = \dfrac{Q' w_{ft} \times L}{MC_p}$$

Now, bulk temperature

$$\begin{aligned}
T_{bx} &= T_i + (\Delta T)_x \\
&= T_i + \dfrac{Q' w_{ft} \times L}{M.C_p} \\
&= 29.5 + \dfrac{1146.826 \times 0.53191 \times x}{0.026979 \times 1014.93} \\
&= 29.5 + 22.27773 \, x \, °C
\end{aligned}$$

$$(B-8)$$

Local convective heat transfer co-efficient is given by

$$h_x = \dfrac{Q'}{(T_w - T_o)_x} = \dfrac{1146.592}{(T_w - T_o)_x} \quad W/m^2 \, °C$$

Local Nusselt number

$$(Nu)_x = \dfrac{h_x D_h}{K} = \dfrac{0.025282 \, h_x}{0.02693} = 0.9388 \, h_x$$

Table B.4 Experimental data of heat transfer of finned tube

X (m)	T_{bx} (°C)	T_{wx} (°C)	h_x (W/m^2.°C)	N_{ux}	$(T_w-T_b)_x$
0.05	30.61	54.31	48.379	45.418	23.7
0.25	35.07	70.49	32.371	30.389	35.42
0.45	39.52	81.92	27.042	25.39	42.4
0.65	43.98	87.17	26.547	24.922	43.19
0.85	48.43	94.59	24.839	23.319	46.16
1.05	52.89	99.23	24.743	23.229	46.34
1.25	57.34	103.88	24.636	23.128	46.54
1.45	61.80	110.05	23.764	22.309	48.25

Average heat transfer coefficient based on inside diameter and nominal area,

$$\bar{h} = \frac{Q}{A(T_{wav} - T_{bav})}$$

$$= \frac{914.82}{(87.705 - 46.205) \times 0.329867}$$

$$= 66.826 \quad W/m^2.\circ C$$

Average Nusselt number based on inside diameter and nominal area,

$$\overline{Nu} = \frac{\bar{h}D_i}{K}$$

$$= \frac{66.826 \times 0.07}{0.02693}$$

$$= 173.7029$$

Pumping Power, $P_m = \frac{\Delta P}{\rho}.M = 2.5835\ W$

DETERMINATION OF LOCATION OF MEASURING INSTRUMENT

PITOT TUBE

For the measurement of velocity head, the tube diameter was divided into five equal concentric areas, and their centeres were found by using Arithmetic mean method. The locations for the traversing pitot is shown in the Fig. 4.7. Arithmetic mean method is given bellow:

$$\frac{1}{5}\pi R^2 = \pi r_1^2$$

$r_1 = 0.447R$

$$\frac{1}{5}\pi R^2 = \pi r_2^2 - \pi r_1^2$$

$$\Rightarrow \frac{1}{5}R^2 + (0.447R)^2 = r_2^2$$

$\therefore r_2 = 0.632R$

Similarly

$r_3 = 0.774R$, $r_4 = 0.894R$, and $r_5 = 1R$

Now

$$\pi r_{5-4}'^2 = \frac{\pi R^2 + \pi(0.894R)^2}{2}$$

$\therefore r_{5-4}' = 0.948R$

$$\pi r'^2 = \frac{\pi(0.894R)^2 + \pi(0.774R)^2}{2}$$

$$\therefore r'_{4-3} = 0.836R$$

Again, Similarly

$r'_{3-4} = 0.7065R$

$r'_{2-1} = 0.547R$

$r'_{1-0} = 0.316R$

THERMOCOUPLE

To find out the location of thermocouple for measurement of outlet air temperature, the tube diameter was divided into three equal concentric areas and then their centers were found out by using an arithmetic mean method. The locations of the thermocouples are shown in the Fig. 4.9. The arithmetic mean method is given below:

$D = 0.07$ m

$r_1 = .035$ m

$A = \pi r_1^2 = .0038485$

$\dfrac{A}{3} = A_1 = A_2 = A_3 = .0012828$

$A_1 = \pi r_1^2 - \pi r_2^2$

$A_2 = \pi r_2^2 - \pi r_3^2$

$A_1 = \pi r_3^2$

$Q_1 = A_1 V \rho C_p (T_{b1} - T_1)$

$Q_2 = A_2 V \rho C_p (T_{b2} - T_1)$

$Q_3 = A_3 V \rho C_p (T_{b3} - T_1)$

$Q = A V \rho C_p (T_{bav} - T_1) = Q_1 + Q_2 + Q_3 = A_1 V \rho C_p (T_{b1} + T_{b2} + T_{b3} - 3T_1)$

$\dfrac{A}{A_1}(T_{bav} - T_1) = (T_{b1} + T_{b2} + T_{b3} - 3T_1)$

$T_{bav} = \dfrac{T_{b1} + T_{b2} + T_{b3}}{3}$

$A_1 = \pi r_1^2 - \pi r_2^2$

$0.0012828 = \pi(0.035)^2 - \pi r_2^2$

$r_2 = 0.0286m$

$A_2 = \pi r_2^2 - \pi r_3^2$

$0.0012828 = \pi(0.0286)^2 - \pi r_3^2$

$r_3 = 0.02024m$

Now,

$$\pi R_1^2 = \frac{\pi r_1^2 + \pi r_2^2}{2}$$

$R_1 = 0.03196$

$$\pi R_2^2 = \frac{\pi r_2^2 + \pi r_3^2}{2}$$

$R_2 = 0.02475$

$R_3 = 0.0143$

$R'_1 = 0.035 - R_1 = 0.00304m$

$R'_2 = 0.035 - R_2 = 0.01025m$

$R'_3 = 0.035 - R_3 = 0.02068m$

Mean outlet temperature was measured by traversing the thermocouple along the **diameter** of the pipe at seven measuring points.

APPENDIX-D

UNCERTAINTY ANALYSIS

Energy measurement contains certain error, so it requires description of inaccuracies. It is generally accepted that an appropriate concept for expressing inaccuracies is an "uncertainty" and that the value should be provided by an "uncertainty analysis". An uncertainty is not the same as an error. An error in measurement is the difference between the true value and the recorded value; an error is a fixed number and can not be a statistical variable. An uncertainty is a possible value that the error might creep into a given measurement. Since uncertainty can take on various values over a range, it is inherently a statistical variable.

1.   Uncertainties in measurands

Now-a-days experimenters are advised to report the uncertainties in every measurand considering the following information:

a.   *Precision limit*, P : This is an estimate of the lack of repeatability caused by random errors and process unsteadiness. This element can be sampled with the available procedure and apparatus, and should be based on statistical estimates from samples whenever possible.

b.   *Bias limit*, B. :   The bias limit is an estimate of the magnitude of the fixed constant error. This element can not be sampled within available procedure and its existence is what mandates the need of cross-checks.

c.   *Uncertainty*, W: The ± 5 interval about the nominal results is the band within which the experiment is 95% confident that the true value of the result lies. And it is calculated from the following:

$$W = |P^2 + B^2|^{1/2} \qquad\qquad (D-1)$$

2.   Propagation of uncertainties into results:

In calibration experiments, one measures the desired result directly. No problem of uncertainty then aries; we have desired results in hand once we complete measurements. In nearly all other experiments, it is necessary to compute the uncertainty in the results from the estimates of uncertainty in the measurands. This computation process is called "propagation of uncertainty".

According to Kline and McClintock (1953), the propagation equation of a result R computed from n measurands $x_1, x_2, x_3 \ldots\ldots x_n$ having absolute uncertainty W_R is given by the following equation:

$$W_R = \left[\left(\frac{\partial R}{\partial x_1} w_{x1} \right)^2 + \left(\frac{\partial R}{\partial x_2} w_{x2} \right)^2 + \ldots\ldots + \left(\frac{\partial R}{\partial x_n} w_{xn} \right)^2 \right]^{1/2} \qquad (D-2)$$

Which can be considered separately in computing the precision and bias components of uncertainties when the function of R is known

3.   Calculation of uncertainties in the present experiment

Results of an uncertainty analysis of the primary measurements (t, b, d, A, T_o, T_i, ΔP, D_i, x) are presented in the following table:

Table 5.1 uncertainties in measurands

Measurands	Precision limit, P	Bias limit, B	Total limit, W
t	1.5%	0.02%	1.50%
b	0	0.013%	0.013%
d	1.05%	3.0%	3.178%
Λ	0	0.52%	0.52%
T_o	1.5%	0.02%	1.50%
T_i	1.5%	0.02%	1.50%
ΔP	5.0%	3.0%	5.83%
D_i	0	0.02%	0.02%
x	0	0.02%	0.02%

Table 5.2 Uncertainties in calculated quantities

Quantity	Total uncertainty
V	1.71%
Q	4.1%
F_i	6.76%

Determination of Mean Velocity:

$$V = 20.558\left(\frac{273+t}{b}\right)^{1/2}(d)^{1/2}$$

Room Temperature

$t = 29.5 \pm 1.50013\%$ ^{o}C

Atmospheric pressure

$b = 741.5 \pm 0.013\%$ mm of Hg

$d = 0.33265 \pm 3.178\%$ cm of fluid

[Since, Mean value of d = 0.33265cm of working fluid]

The uncertainty in this value is calculated as follows. The various terms are:

$w_t = 0.4425$ ^{o}C

$w_b = 0.1$ mm of Hg

$w_d = 0.01057$ cm of fluid

Change of velocity with respect to temperature

$$\frac{\partial V}{\partial t} = 20.558 \times \frac{1}{2}\left(\frac{273+t}{b}\right)^{-1/2} \frac{1}{b}(d)^{1/2}$$

$$= 20.558 \times \frac{1}{2}\left(\frac{273+29.5}{741.5}\right)^{1/2} \frac{1}{741.5}(0.33265)^{1/2}$$

$$= 0.0125177$$

Change of velocity with respect to Atm. pressure

$$\frac{\partial V}{\partial b} = 20.558 \times \frac{1}{2}\left(\frac{273+t}{b}\right)^{1/2}(273+t)b^{-3/2}(d)^{1/2}$$

$$= 20.558 \times \frac{1}{2}\left(\frac{273+29.5}{741.5}\right)^{1/2}(273+29.5)(741.5)^{-3/2}(0.33265)^{1/2}$$

$$= 0.139058$$

Change of velocity with respect to manometric head

$$\frac{\partial V}{\partial d} = 20.558\left(\frac{273+t}{b}\right)^{1/2}\frac{1}{2}(d)^{-1/2}$$

$$= 20.558\left(\frac{273+29.5}{741.5}\right)^{1/2}\frac{1}{2}(0.33265)^{-1/2}$$

$$= 11.3832$$

Thus, the uncertainty in the velocity is

$$w_v = \left[\left(\frac{\partial V}{\partial t}w_t\right)^2 + \left(\frac{\partial V}{\partial b}w_b\right)^2 + \left(\frac{\partial V}{\partial d}w_d\right)^2\right]^{1/2}$$

$$= \left[(0.0125177 \times 0.4425)^2 + (0.139058 \times 0.1)^2 + (11.3832 \times 0.01057)^2\right]^{1/2}$$

$$= 0.12125 \text{ m/s}$$

Now, $\dfrac{w_v}{v} = \dfrac{0.12125}{7.0878} = 1.71\%$

Total Heat input to the air

Q = MC$_p$(T$_o$ - T$_i$)

Q = ρA$_s$VC$_p$(T$_o$ - T$_i$)

A$_s$ = 0.0038485 ± 0.52%

V = 7.0878 ± 1.71%

T$_o$ = 54.71 ± 1.50013%

T$_i$ = 29.5 ± 1.50013%

The uncertainty in this value is calculated as follows.

The various terms are:

$$w_A \quad 0.00002$$

$$w_V = 0.12125$$

$$w_{T_o} = 54.71 \times 0.150013 = 0.82072$$

$$w_{T_i} = 29.5 \times 0.0150013 = 0.44254$$

Change of total heat input with respect to area

$$\frac{\partial Q}{\partial A} = \rho V C p (T_0 - T_i)$$

$$= 1.1689 \times 7.9878 \times 1006.69 \times (54.71 - 29.5)$$

$$= 0.21017 \times 10^6$$

Change of total heat input with respect to velocity

$$\frac{\partial Q}{\partial V} = \rho A C_p (T_0 T_i)$$

$$= 1.1684 \times 0.0038485 \times 1006.69 (54.71 - 29.5)$$

$$= 114.1173$$

Change of total heat input with respect to outlet temperature

$$\frac{\partial Q}{\partial T_0} = \rho A V C_p$$

$$= 1.1684 \times 0.0038485 \times 7.0878 \times 1006.69$$

$$= 32.08412$$

Change of total heat input with respect to inlet temperature

$$\frac{\partial Q}{\partial T_i} = -\rho A V C_p$$

$$= -1.1684 \times 0.0038485 \times 7.0878 \times 1006.69$$

$$= -32.0841$$

Thus, the uncertainty in the Total Heat Input to the air

$$w_Q = \left[\left(\frac{\partial Q}{\partial A} w_A\right)^2 + \left(\frac{\partial Q}{\partial V} w_V\right)^2 + \left(\frac{\partial Q}{\partial T_0} w_{To}\right)^2 + \left(\frac{\partial Q}{\partial T_i} w_{Ti}\right)^2\right]^{1/2}$$

$$= 33.2279 \text{ W}$$

Now $\quad \dfrac{w_Q}{Q} = \dfrac{33.2279}{808.843} = 4.1\%$

Friction Factor:

Local friction factor based on inside diameter is given by

$$F_i = \frac{2(\Delta P / x) D_i}{\rho V^2}$$

$\Delta P = 5.37 \pm 5.83\%$

$x = 0.05 \pm 0.02\%$

$D_i = 0.07 \pm 0.02\%$

$V = 7.0878 \pm 1.71\%$

$w_{\Delta P} = 0.313071$

$w_x = 0.00001$

$w_{Di} = 0.00001$

$w_V = 0.1212$

Change of friction factor with respect to pressure drop

$$\frac{\partial F_i}{\partial \Delta P} = \frac{2D_i}{\rho V^2 x} = \frac{2 \times 0.07}{1.1684 \times (7.0878)^2 \times 0.05} = 0.047702$$

Change of friction factor with respect to axial distance

$$\frac{\partial F_i}{\partial x} = \frac{-2\Delta P D_i}{\rho V^2 x^2} = \frac{-2 \times 5.37 \times 0.07}{1.1684 \times (7.0878)^2 \times (0.05)^2} = 5.123$$

Change of friction factor with respect to inside diameter

$$\frac{\partial F_i}{\partial D_i} = \frac{2\Delta P}{\rho V^2 x} = \frac{2 \times 5.37}{1.1684 \times (7.0878)^2 \times 0.05} = 3.659$$

Change of friction factor with respect to velocity

$$\frac{\partial F_i}{\partial V} = -2\frac{\Delta P D_i (2)}{\rho V^3 x} = \frac{-4(5.37) \times 0.07}{1.1684 \times (7.0878)^3 \times 0.05} = -0.0722$$

Thus, the uncertainty in the Friction factor

$$w_{F_i} = \left[\left(\frac{\partial F_i}{\partial \Delta P} w_{\Delta P} \right)^2 + \left(\frac{\partial F_i}{\partial X} w_x \right)^2 + \left(\frac{\partial F_i}{\partial D_i} w_{D_i} \right)^2 + \left(\frac{\partial F_i}{\partial V} w_v \right)^2 \right]^{\frac{1}{2}}$$

$$= \left[\begin{array}{l} (0.047702 \times 0.313071)^2 + (5.123 \times 0.00001)^2 + (3.659 \times 0.00001)^2 \\ + (0.0722 \times 0.12125)^2 \end{array} \right]^{\frac{1}{2}}$$

$$= 0.01731$$

Now, $\dfrac{w_{F_i}}{F_i} = \dfrac{0.01731}{0.256} = 6.76\%$

APPENDIX-E

EXPERIMENTAL DATA

DATA FOR SMOOTH TUBE

Pressure drop, ΔP (N/m^2)

X/L	Re				
	19139	29165	40005	47445	50379
0.033333	5.85	5.37	2.9	2.44	1.95
0.166667	11.23	10.26	4.39	4.39	3.91
0.3	15.63	13.68	8.31	5.96	5.37
0.433333	20.02	17.1	11.23	7.33	6.84
0.566667	24.42	20.52	13.68	9.28	8.012
0.7	27.84	21.98	15.14	10.75	8.99
0.833333	30.58	22.47	16.12	11.72	9.87
0.966667	32.24	23.45	16.61	12.21	10.75

Friction factor, F (-)

X/L	Re				
	19139	29165	40005	47445	50379
0.033333	0.16175	0.064	0.01865	0.01098	0.00775
0.166667	0.06225	0.02445	0.00558	0.00395	0.00313
0.3	0.048	0.01812	0.00585	0.00298	0.00238
0.433333	0.04275	0.01567	0.00548	0.00253	0.0021
0.566667	0.03975	0.0144	0.0051	0.00245	0.00188
0.7	0.0365	0.01247	0.00458	0.0023	0.0017
0.833333	0.03375	0.0107	0.00408	0.00213	0.00158
0.966667	0.03075	0.00965	0.00363	0.0019	0.00148

Wall temperature, $T_{wx}(^{o}C)$

X/L	Re				
	19139	29165	40005	47445	50379
0.033333	72.39	68.59	60.39	58.51	57.46
0.166667	86.06	76.71	68.66	65.06	63.72
0.3	112.01	98.83	87.36	82.01	80.36
0.433333	129.68	121.77	107.78	102.79	101.56
0.566667	133.45	125.94	111.08	105.33	103.82
0.7	128.24	123.43	109.38	103.47	102.25
0.833333	124.39	121.53	107.22	102.62	101.19
0.966667	111.87	110.77	98.82	95.31	93.88

Bulk temperature, $T_{bx}(^{o}C)$

X/L	Re				
	19139	29165	40005	47445	50379
0.033333	30.357	30.34	30.16	30.116	30.081
0.166667	33.785	33.7	32.8	32.582	32.405
0.3	37.213	37.06	35.44	35.047	34.729
0.433333	40.641	40.42	38.08	37.512	37.053
0.566667	44.069	43.76	40.73	39.978	39.377
0.7	47.497	47.15	43.37	42.44	41.701
0.833333	50.925	50.51	46.01	44.91	44.025
0.966667	54.353	53.87	48.65	47.374	46.349

Local heat transfer coefficient, h_x $(W/m^{2\,o}C)$

X/L	Re				
	19139	29165	40005	47445	50379
0.033333	39.04	64.109	87.44	103.04	106.96
0.166667	31.39	57.014	73.71	90.083	93.515
0.3	21.94	39.6984	50.91	62.298	64.176
0.433333	18.43	30.143	37.92	44.819	45.397
0.566667	18.36	29.8388	37.57	44.768	45.442
0.7	20.325	32.147	40.04	47.94	48.365
0.833333	22.34	34.528	43.18	50.697	51.227
0.966667	28.53	43.096	52.69	61.03	61.61

Local Nusselt number, $Nu_x(-)$

X/L	Re				
	19139	29165	40005	47445	50379
0.033333	99.81	163.901	223.55	265.43	273.45
0.166667	80.25	145.762	188.45	230.306	239.08
0.3	56.09	101.492	130.16	159.27	164.07
0.433333	47.12	77.064	96.95	114.58	116.06
0.566667	46.94	76.286	96.05	114.45	116.17
0.7	51.96	82.187	102.37	122.563	123.65
0.833333	57.11	88.274	110.39	129.61	130.97
0.966667	72.94	101.179	134.707	156.029	157.51

Heat transfer coefficient, h, Nusselt number , Nu (-) and Pumping Power, Pm

Re (-)	h $(W/m^2{}^\circ C)$	Nu (-)	Pm (W)
19139	25.044	64.028	0.5771
29165	38.343	98.0267	0.6396
40005	52.934	135.33	0.6215
47445	63.0845	161.282	0.5418
50379	64.586	165.122	0.5065

DATA FOR FINNED TUBE

Pressure drop, ΔP (N/m^2)

X/L	Re				
	22110	29004	39425	44028	45434
0.033333	16.05	15.631	13.37	12.43	9.94
0.166667	40.3817	34.285	30.735	21.873	20.894
0.3	53.77	43.964	37.66	28.83	27.37
0.433333	67.83	52.664	45.08	37.304	36.355
0.566667	81.62	71.314	60.11	50.389	42.952
0.7	96.76	84.014	75.55	65.89	55.964
0.833333	113.81	97.69	85.89	67.29	56.876
0.966667	120.66	102.58	87.05	68.496	60.59

Friction factor, F (-)

X/L	Re				
	22110	29004	39425	44028	45434
0.033333	0.316	0.1788	0.0865	0.0649	0.0488
0.166667	0.15	0.0705	0.0398	0.0228	0.0205
0.3	0.117	0.0568	0.027	0.0167	0.0149
0.433333	0.103	0.0525	0.0244	0.0149	0.0134
0.566667	0.0944	0.0488	0.0228	0.0155	0.0124
0.7	0.091	0.0466	0.0233	0.0163	0.0131
0.833333	0.0895	0.0451	0.0222	0.0141	0.0112
0.966667	0.0818	0.0439	0.0194	0.0123	0.0103

Wall temperature, T_w (^{o}C)

X/L	Re				
	22110	29004	39425	44028	45434
0.033333	58.52	54.31	46.63	45.27	45.03
0.166667	76.15	70.49	61.14	56.99	55.8
0.3	85.48	81.92	67.62	65.82	63.06
0.433333	97.06	87.17	72.47	69.22	67.2
0.566667	102.65	94.59	76.27	73.49	72.15
0.7	108.52	99.23	79.99	76.98	75.79
0.833333	113.74	103.88	83.57	80.71	79.02
0.966667	119.41	110.05	87.38	84.51	82.44

Bulk temperature, T_{wx} (°C)

X/L	Re				
	22110	29004	39425	44028	45434
0.033333	30.79	30.61	30.37	30.308	30.287
0.166667	35.94	35.07	33.85	33.54	33.43
0.3	41.09	39.52	37.35	36.772	36.586
0.433333	46.24	43.43	40.83	40.004	39.74
0.566667	51.39	48.43	44.32	43.236	42.88
0.7	56.55	52.89	47.81	46.468	46.034
0.833333	61.69	57.34	51.3	49.7	49.183
0.966667	66.85	61.8	54.79	52.932	52.33

Fin tip temperature, T_{tx} (°C)

X/L	Re				
	22110	29004	39425	44028	45434
0.033333	53.79	50.84	44.97	42.27	40.92
0.166667	71.01	66.96	57.63	57.03	55.29
0.3	83.75	74.86	60.21	58.03	57.19
0.433333	88.78	83.06	66.49	64.05	62.93
0.566667	96.51	90.06	71.32	68.66	64.3
0.7	98.63	91.15	70.99	70.1	66.61
0.833333	104.64	97.16	75.91	72.89	71.18
0.966667	110.66	103.29	80.52	77.01	75.15

Local heat transfer coefficient, h_x (W/m^2 °C)

X/L	Re				
	22110	29004	39425	44028	45434
0.033333	36.66	48.379	74.31	83.56	85.21
0.166667	25.28	32.371	44.28	53.31	56.16
0.3	24.74	27.042	39.92	43.03	47.45
0.433333	21.985	26.547	38.19	42.79	45.75
0.566667	19.78	24.839	37.82	41.32	42.92
0.7	17.976	24.743	37.55	40.97	42.22
0.833333	16.479	24.636	37.45	40.31	42.103
0.966667	15.207	23.764	37.07	39.59	41.722

Local Nusselt number, $Nu_x(-)$

X/L	Re				
	22110	29004	39425	44028	45434
0.033333	34.178	45.418	70.41	79.38	81.01
0.166667	23.57	30.389	41.96	50.64	53.39
0.3	23.06	25.39	37.83	40.88	45.11
0.433333	20.49	24.922	36.188	40.65	43.49
0.566667	18.44	23.319	35.84	39.25	40.81
0.7	16.759	23.229	35.58	38.97	40.14
0.833333	15.36	23.128	35.48	38.29	40.03
0.966667	14.17	22.309	35.13	37.61	39.67

Heat transfer coefficient, h, Nusselt number, Nu (-), Pumping Power, Pm and Performance Parameter, R

Re (-)	h (W/m^2°C)	Nu (-)	Pm (W)	R (-)
22110	53.023	136.873	2.3479	2.3479
29004	66.826	173.703	2.5835	2.5835
39425	99.729	261.653	2.925	2.925
44028	109.941	289.173	2.5575	2.5575
45434	115.743	304.68	2.331	2.331